Long-Range Forecasting and Climate Research

General circulation model simulations using cloud distributions from the GAPOD satellite data archive and other sources

by

R. Swinbank

LRFC 13

May 1987

LONG RANGE FORECASTING AND CLIMATE
RESEARCH MEMORANDUM NO. 13

GENERAL CIRCULATION MODEL SIMULATIONS USING CLOUD DISTRIBUTIONS FROM THE GAPOD SATELLITE DATA ARCHIVE AND OTHER SOURCES

by

R. SWINBANK

MET O 13 (SYNOPTIC CLIMATOLOGY BRANCH)
METEOROLOGICAL OFFICE
LONDON ROAD
BRACKNELL
BERKSHIRE RG12 2SZ

MAY 1987

General circulation model simulations using cloud distributions from the GAPOD satellite data archive and other sources

by R. Swinbank

1. Introduction

The aim of this paper is to assess the impact of varying the cloud distribution used in general circulation model simulations, and in particular to assess the desirability of using cloud data derived from satellite observations. This paper describes the results from several parallel integrations of the 11-layer General Circulation Model (Slingo, 1985), each run for 3 months (December to February). In the past, the cloud distribution used by the interactive radiation scheme of the model was zonally symmetric, and based on cloud amounts observed climatologically. More recently, a fully interactive cloud/radiation scheme has been developed, so that the clouds used depend on model parameters (in particular humidity). Both schemes are featured in model simulations studied in this paper. In addition an experiment has been run in which the cloud distribution was derived from GAPOD satellite cloud data. (GAPOD is the Met O 13 Global Archive of Polar Orbiter Data.) A further two experiments - one with no cloud, and one with an idealised cloud distribution - are also described.

The Met O 20 11-layer GCM is a global finite difference model developed for the Cyber 205 from the model originally described by Saker (1975). It incorporates parametrizations of boundary layer and surface exchange processes, convection, large-scale precipitation and radiation, as described by Slingo (1985). Also included is a scheme to parametrize orographically induced gravity wave drag (Palmer et al., 1986). From the point of view of this project, the most crucial scheme is the interactive radiation scheme. In this scheme layer cloud may exist at three levels (high, medium and low), each of which is taken to be one model layer deep. Convective cloud, extending over several layers, may also be present. In the shortwave spectral region the scheme takes into account absorption by minor constituents. The longwave radiation scheme has been described by Slingo and Wilderspin (1986) and includes atmospheric absorption and emission due to water vapour, carbon dioxide and ozone in seven different wave-bands. The shortwave reflectivity, absorptivity and transmittivity of each cloud type are prescribed (table 4.1 of Slingo (1985)); in the infra-red medium and low clouds are treated as black bodies, while the emissivity of high cloud is 0.75.

For each integration, the initial conditions for the model were

derived from the Met Office operational analysis for 0Z on 30th November 1983. The model runs were each 90 days long (three 30-day months), with seasonally varying radiation. The cloud distributions also varied to some degree through the integrations; further details of the cloud distributions are given in section 2. Results from a previous pair of integrations, one using zonally symmetric climatological cloud, and the other using cloud amounts from the GAPOD archive have previously been reported by Swinbank (1985) (hereafter referred to as S). These experiments were both 60-day non seasonally varying integrations (using radiation appropriate to mid-January); the satellite clouds were derived from January 1983 data and the last 30 days of each integration were analysed. Section 3 describes some of the results from the present set of 90-day simulations and compares them to the earlier experiments. Finally, in section 4, the results are discussed and the future use of GAPOD cloud data in general circulation model experiments is considered.

2. Cloud distributions

a. Zonally symmetric climatology

In the first experiment (C1) the GCM was run using prescribed zonally symmetric cloud amounts and heights. The cloud distribution was as normally used for the 11-layer model integrations which do not incorporate interactive cloud. The cloud amounts and levels are defined on a 10 degree latitude grid for mid-January, April, July and October (see tables 4.2 and 4.3 of Slingo (1985)). To derive the cloud amounts used in the model the data are first interpolated to the model grid rows. The cloud amounts are held constant for 15 days on either side of the middle of the above months, and at other times are linearly interpolated from the values given. The cloud heights are assigned the value from the month which is closest to the model date. Graphs of the zonally symmetric cloud amounts (averaged over 90 days) are shown in Fig 1, along with the zonal means of the other cloud distributions, as described below. The cloud amount and cloud base data for January are shown in Figs 2 and 4 of S.

b. GAPOD cloud distribution

For experiment C2, the cloud distribution was based on the GAPOD satellite cloud data for the months of December 1983 to February 1984; each month of the integration used different cloud amounts, calculated from the corresponding monthly GAPOD data. The method used to derive the cloud distributions is essentially as described in section 2 of S and by Lunnon (1983). The procedure converts the GAPOD data, which

includes total cloud amount and a cloud top temperature distribution at a 5 degree latitude resolution, to the layer cloud amounts, plus the amount of convective cloud, on a 10 degree (latitude) by 15 degree (longitude) grid. In the previous experiments, reported by S, all model grid points within each 10° x 15° box used the appropriate cloud amounts. In this work the data has been smoothed, after being copied to the model points, using a Gaussian filter of half-width 2° latitude (as originally suggested by Sardeshmukh and Hoskins (1984)). The cloud levels were exactly the same as for the zonally symmetric distribution.

90-day mean maps of the cloud amounts (ie. incorporating data from December 1983 to February 1984) are shown in Fig 2. Zonal mean values are also given in Fig 1. This shows that the zonal mean cloud amounts from the GAPOD data follow the climatological data quite closely; although the GAPOD data were derived with the aid of the climatological data there was no absolute constraint that the zonal mean values should be preserved. In all three months the total GAPOD cloud amount is increased over the N hemisphere oceans, the tropical W Pacific, and the eastern parts of the continents (Fig 2e). The bulk of the N hemisphere continental areas have decreased cloud amounts. Elsewhere, and in the southern hemisphere, the changes were generally slight. By level, the high cloud (Fig 2a) generally showed only slight changes, except for an increase of 0.2 over Indonesia; the medium level cloud amounts (Fig 2b) showed large increases over the N Atlantic, and to a lesser extent in the N Pacific. The low cloud amount (2c) has also increased in the western N Atlantic, but also decreased over much of the N hemisphere land areas. Convective amounts (2d) have increased over tropical areas (eg. W Pacific), otherwise the changes are quite patchy.

c. Interactive clouds

For experiment C3 the cloud amounts are calculated each time the radiation scheme is called (every 3 hours). The interactive cloud scheme calculates convective cloud amounts, bases and tops from the saturated mass flux calculated in the convection scheme. Compared with the other experiments in this series, this run had a slightly modified convection scheme incorporating split final detrainment. That is, if a convective parcel enters a stable layer which it cannot completely penetrate, a fraction of the parcel is allowed to penetrate to the next layer; this modification allows some simulation of the effects of trade-wind cumulus on the boundary layer. The relative humidity of each model layer is adjusted to represent the value for the environmental air outside the (saturated) convective tower, if appropriate. Layer cloud amounts are then calculated as a quadratic function of the relative humidity in excess of some prescribed threshold value. These layer

clouds are calculated on the basis of the maximum amounts in specified ranges of model layers: in this case layers 11 to 9 for low cloud, 8 to 6 for medium, and 5 to 2 for high. So, if the cloud amounts calculated for layers 11, 10 and 9 are 0.5, 0.6 and 0.4 respectively, the low cloud amount will be 0.6 and be assigned to layer 10. For further details about the cloud scheme see Slingo and Wilderspin (1985).

The time-mean cloud distributions generated by the interactive cloud scheme are shown in Fig 3, with zonal mean data in Fig 1. Note that, because the cloud amounts generated will vary each time the scheme is called, they are not strictly directly comparable with the amounts in the other experiments. Compared to the GAPOD amounts, the large values of low and medium cloud cover (Figs 3b and 3c) over the N hemisphere oceans are much less marked, but the cloud cover over the N hemisphere continents is significantly increased (and is also much more than for experiment C1). The decrease in maritime layer cloud amount is offset by an increase in the amount of cloud resulting from shallow convection (Fig 3c). The amount of high cloud in the northern hemisphere is greatly increased. The changes in the tropics and S hemisphere are less coherent.

Of the three cloud distributions, the GAPOD should have the advantage of being most realistic, because it is derived from the polar orbitting satellite observations. However it should be borne in mind that the satellite cloud data was originally produced as an indicator of the reliablity of the sounding data, without any guarantee of its absolute accuracy. The interactive cloud data has the advantage that the cloud cover used by the radiation scheme should be well related to the particular synoptic situations simulated by the GCM, rather than being fixed for a long period (or only slowly varying).

d. Idealised cloud distributions

In order to elucidate the results from the previous simulations, a further pair of integrations was run with highly idealised cloud distributions. In experiment C4 all cloud amounts used by the radiation scheme were set identically to zero. In C5 the cloud was restricted to a circular area centred on 60 N, 50 W, of radius equivalent to 20 degrees latitude. For grid boxes centred within a radius of 15° the cloud amounts were 0.8 for low cloud, 0.7 for medium and 0.2 for high (with no convective cloud); between 15° and 20° the cloud amounts varied linearly. As an example, the low cloud distribution is shown in Fig 4. These cloud amounts were intended to mimic the north-south gradient of cloud in the GAPOD data around Nova Scotia, but at the same time avoiding the complexities of the GAPOD distribution.

3. Experiment Results

This section comprises a description of some of the results from the model simulations. First of all, the results of experiments C1, C2 and C3 (with zonally symmetric, GAPOD, and interactive clouds respectively) will be described together. The simulations will also be compared with atmospheric circulation data from the Met O 20 spectral archive of operational analyses (Swinbank, 1983). Finally some results from the simulations with idealised cloud distributions (C4 and C5) will be discussed and compared with the more realistic simulations.

Zonal mean cross-sections of westerly wind components and temperatures for experiments C1 to C3 are given in Figs 5a to c; the corresponding data from the analysis archive are in Fig 5d. Southerly wind components are shown in Fig 6. Comparing Figs 5a and 5d shows that C1 gives a reasonable simulation of the zonal mean fields. The model simulation does not close off the jet in the northern hemisphere stratosphere (and also to a lesser extent in the S hemisphere). The northern hemisphere westerlies are generallly too weak at upper levels north of about 45 N. The cross-sections of meridional wind show that the model Hadley circulation is too weak (compare Figs 6a and 6d). With clouds from the GAPOD data (C2; Figs 5b, 6b) the main change in temperature is an increase at low levels at high northern latitudes (but only by about 3K), this is associated with a further weakening of zonal wind at high latitudes. (These changes are in fact in the opposite sense to those shown in S for fixed January experiments; the differences may result either from random variations, or could reflect changes made to the model.) In the tropics the zonal mean wind has changed from slightly easterly to slightly westerly; the Hadley circulation has improved, but is still too weak. Experiment C3, with interactive radiation, gives probably the least satisfactory zonal mean fields (Figs 5c, 6c). There is no sign of a polar night jet and the southern hemisphere mid-latitude jet also penetrates too high. In the troposphere the zonal wind is similar to the other experiments. Associated with these large errors in upper level wind the temperatures are warmer near and above the tropopause. The temperatures at all levels are generally slightly high, particularly over the North Pole.

The northern hemisphere sea level pressure distributions for the three experiments and as analysed are shown in Fig 7. Experiment C1, with zonally symmetric clouds, gives results that are similar to the analyses. The main difference is that the model has insufficiently high pressure in the Siberian anticyclone. In the southern hemisphere (not

shown) the simulated circumpolar trough is too shallow. Experiment C2 also gives a satisfactory simulation of the atmospheric circulation, with comparatively small differences from C1. Compared to the earlier experiment, the Icelandic and Aleutian lows in C2 are shifted too far west; this is probably associated with increased low cloud amounts over the east coasts of the continents. There is also a general increase of pressure over Asia and western N America, which correlates with decreased low cloud amounts. The fixed January runs in S also showed a slight tendency towards a deeper trough west of Iceland, but in those integrations the main low centre was much too far north-east (because of the lack of gravity wave drag in those experiments). Although there is a small increase in pressure over the NE Atlantic in C2, this is very much smaller than that found in S; in the earlier work, the experiment using GAPOD cloud had an Atlantic storm-track that was shifted east and intensified compared to the control run, while in the present work the two simulations give very similar results. Figure 8 comprises fields showing the RMS variation of high-pass filtered 500 mb height, which is an indicator of the storm tracks (Blackmon 1976). C1 and C2 give similar results in the Atlantic; in each case the RMS amplitude is reduced by about a third compared to that observed (or by about a half in terms of variance). This reduction is also apparent in the southern hemisphere (not shown). The differences between the two experiments were more marked in the Pacific storm-track. The overall intensity is higher in C1, particularly west of the dateline; this difference is probably related to a deeper trough in the Gulf of Alaska in C1. In C2 the storm-track is less intense in the NW Pacific, but extends further east over W Canada.

The simulation of sea level pressure by experiment C3 (Fig 7c) was similar, but with a deeper Aleutian and Icelandic low, shifted further south. In fact in this experiment there is a decrease in pressure over much of the mid-latitudes, which is compensated for in the southern hemisphere. The amplitude of the baroclinic eddies in C3 is indicated by Fig 8c. The amplitude is larger in the Atlantic and the area of storm-track activity is more extensive in the Pacific, so that C3 is intermediate between the two other experiments and the observed eddy activity. Shukla and Sud (1981) have also run two parallel GCM experiments, one with interactive cloud and one with fixed cloud cover. Although their experiments were for N hemisphere summer conditions, they also found a significant difference in eddy activity. Specifically they found that, with vaying cloud amounts, there was a decrease in stationary wave amplitude at 50° N and an increase in variance of waves of period up to 7 days at wavenumbers 6 - 10; they attribute this to an increase in baroclinic wave activity. These results imply that, for the simulation of baroclinic wave activity, it is advantageous to calculate

the cloud amounts interactively.

As reported in S, the differences found in sea level pressure were reflected in differences in the height fields at upper levels. Maps of the 500 mb height fields are shown in Fig 9. The results show a good simulation of 500 mb height by experiment C1, apart from a systematic low bias of a few decametres relative to the analyses (probably related to the way in which height fields are calculated from the model variables). Experiment C2 has a ridge/trough pattern near the Greenwich meridian that is probably slightly too strong. C3 is similar to C2, but with slightly larger values in the vortex centre (cf. the temperature differences mentioned above).

Figure 10 shows the simulations of sea level pressure for the two simulations with no cloud (C4) and the idealised cloud distribution (C5), together with the difference (C5 minus C4). Both experiments give results which are at least superficially similar to the observed atmospheric circulation (Fig 3d). Thus the differences between these idealised runs should be a reliable indicator of the effect of cloud in more realistic experiments. The main differences from the observed circulation is that in both cases the Icelandic low is split into one centre south of Greenland and one north of Norway, and the Aleutian low is also more clearly split than in the observed data. The Azores high pressure area is also shifted somewhat eastwards, with ridging over S Europe. It is somewhat surprising that these experiments, with little or no cloud, give results that are similar to the observed atmospheric circulation. In an earlier study Hunt (1978) also ran a GCM experiment removing the radiative effects of clouds. That study used a hemispheric model with no topography and 'annual mean' radiation. Hunt also found that the effect of omitting clouds was generally small; the main consequence of omitting cloud was a warming of the lower troposphere. This behaviour was attributed to feedback mechanisms, for example convection, that tended to minimise the changes to the general circulation as a whole. In the present study the effect of cloud is generally to warm the lower troposphere; this is probably because the main effect of low cloud in winter is to block the outgoing longwave radiation rather than the incoming radiation. This is shown clearly in Fig 11a (and also in results given in S), though Fig 11b shows the situation is not neccessarily clear-cut. Yagai (1986), for summer integrations, reported that increased cloud amounts led to increased low level temperatures.

The difference in sea level pressure between experiments C4 and C5 is rather small (Fig 10c). The results from C5 do show an increase in pressure over Greenland (which was under the cloudy area - Fig 4) with

a decrease over the central N Atlantic (mainly to the south of the cloudy area). In S the intensity of the storm tracks was quite well related to the meridional temperature gradient in the neighbourhood of the start of the storm tracks. For experiment C5, the temperature differences at 850 mb (Fig 11a) show a general warming in the cloudy area, with an implied reduction in baroclinity. Maps of the 'storm-tracks' for the two experiments are in Fig 12. The difference in baroclinity is consistent with the slightly weaker storm-track and reduced low level westerly flow in C5, as compared to C4. However at 700 mb (Fig 11b) C5 shows a general cooling in the NW Atlantic, with little change (if anything a slight increase) in temperature gradient near Nova Scotia. Further downstream C5 has increased pressure over Europe, with a small decrease west of Norway. The pressure changes in the rest of the globe are likely to be less significant because they are further from the cloudy area. Although there are relatively large changes in pressure over Siberia and the N Pacific, there are also similar changes in the southern hemisphere, which one would expect to be largely unaffected. The fact that such changes are found at a large distance from the cloudy area may indicate some teleconnectivity in the model, or (more likely) may just show that the differences resulting from the cloud cover are not of large enough amplitude to be readily distinguished from random variability. The equivalent 500 mb maps are in Fig 13; the difference map is very similar to that for sea level pressure.

Thus, at high winter latitudes, one would expect that the effect of cloud would be to increase temperatures in the lower troposphere. Although the results in S follow this pattern (as do the idealised cloud runs), the results from the other experiments are not so clear-cut. Fig 14 shows differences between experiments C2 and C1 for cloud amount, 700 mb temperature sea level pressure and 500 mb height. As mentioned in section 2, the cloud increases over the oceans result from low and medium layer clouds (compare Figs 14a with Figs 2b,c). These changes are not well correlated with the 700 mb temperature differences, but in turn these differences (at both 700 mb and 850 mb) are very well correlated with changes at sea level and 500 mb (Figs 14b,c and d). In S the cloud amount changes were well correlated with all three of these fields. The cloud amount changes in the Atlantic 'storm- track' area were found to have large downstream effects; this was illustrated by the differences in the eddy forcing of the 250 mb streamfunction field. In this study the differences were rather smaller, and not so clearly related to the changes in cloud distribution.

4. Discussion

One of the reasons for running the 90-day experiments was to ascertain whether the differences found in S were a result of the different cloud distributions, or whether they could be attributed to random variations. As remarked earlier, the differences within the present set of experiments is generally less than found in the earlier study. That work was based on 30-day means from fixed January integrations, while the present study is based on 90-day December - February simulations. Because of the shorter period, random variations would be expected to give larger differences in the first case. In the present work, each month has slightly different satellite cloud data, which would also tend to smooth out any differences (and for the interactive cloud experiment any cloud related differences may be further blurred). In S large blocks of grid points were assigned the same cloud cover, leading to sharp gradients in cloud amounts; this may have led to unduly large temperature gradients and unrealistic changes to the simulated atmospheric circulation. There may also be differences in the effect of cloud due to changes in the 11-layer model between the two studies (the main changes being the revised longwave radiation scheme and the introduction of gravity wave drag). These considerations lead one to expect that the response may not be as large in the present simulations. One is led to conclude that the effect of cloud amount on atmospheric circulation, as judged using the present 11-layer model, is relatively small. This conclusion is backed up by the two experiments (C4 and C5), which although their cloud distributions were radically different from observed distributions, gave simulations that were very similar to one another and not dissimilar to the observed atmospheric circulation.

From the current set of experiments it is not possible to say whether this small impact is realistic, or whether it is affected by shortcomings in the treatment of cloud by the model radiation scheme. The fact that other workers have found effects of similar magnitude in other general circulation models implies that the experiments do give a realistic indication of the sensitivity of the atmospheric circulation to cloud cover.

A principal motivation for the GAPOD project was to provide realistic cloud distributions based on satellite data, for use in long range dynamical forecasts. As an alternative to using a zonally symmetric cloud distribution, it is obviously preferable to use more realistic cloud amounts, such as a climatological distribution derived from several years of GAPOD data. However, since the GAPOD project has

been running, an interactive cloud scheme has been developed for the 11-layer GCM (as used in experiment C3). This has avoided the need to use the inherently undesirable zonally symmetric cloud distribution, and instead model cloud amounts can be better related to the actual simulated model circulation. Calculating cloud amounts interactively also has the beneficial effect of increasing the simulated baroclinic wave activity. However, there are some shortcomings in the model simulation of clouds, and some associated errors in the simulated circulation (particularly at high levels). The present simulations to study the effect of cloud distributions do not show a large effect on the model simulations (much less than, for example, the effect of incorporating gravity wave drag). The results do not show that any of the three types of cloud distribution is clearly better (or worse) than any other. Thus there seems little justification in pursuing the GAPOD project as a means to derive cloud data for the long range forecast experiments. Rather, it would be preferable to continue to use the interactive cloud scheme in the dynamical forecast experiments.

References

M.L. Blackmon	1976	A climatological spectral study of the 500mb geopotential height of the northern hemisphere. *J. Atmos. Sci.* **33**, 1607-1623
B.G. Hunt	1978	On the general circulation of an atmosphere without clouds. *Quart. J. R. Met. Soc.*, **104**, 91-102.
R.W. Lunnon	1983	The derivation of 11-layer model cloud distribution parameters from GAPOD data. *Unpublished manuscript.*
T.N. Palmer, G.J. Shutts and R. Swinbank	1986	Alleviation of a systematic westerly bias in general circulation and numerical weather prediction models through an orographic gravity wave drag parametrization. *Quart. J. R. Met. Soc.*, **112**, 1001-1039.
N.J. Saker	1975	An 11-layer general circulation model. Met O 20 Tech. Note II/70.
P.D. Sardeshmukh and B.J. Hoskins	1984	Spatial smoothing on a sphere. *Mon. Wea. Rev.*, **112**, 2524-2529.
J. Shukla and Y.Sud	1981	Effect of cloud-radiation feedback on the climate of a general circulation model. *J. Atmos. Sci.*, **38**, 2337-2353
A. Slingo (Ed.)	1985	Handbook of the Meteorological Office 11-layer atmospheric general circulation model, Vol 1: Model description. Dynamical Climatology Technical Note no. 29.
A. Slingo and R.C. Wilderspin	1985	Simulation of cloudiness with the UK Meteorological Office 11-layer AGCM. Dynamical Climatology Technical Note no. 22.
A. Slingo and R.C. Wilderspin	1986	Development of a revised longwave radiation scheme for an atmospheric general circulation model. *Quart. J. R. Met. Soc.*, **112**, 371-386

R. Swinbank 1983 A system to archive operational analyses for research purposes. Met O 20 Tech. Note no. II/218.

R. Swinbank 1985 Interim report on General Circulation Model experiments using cloud distributions derived from GAPOD data. Met O 13 Branch Memorandum no. 158.

I. Yagai 1986 The effect of clouds on the medium range weather forecasting. *Research activities in atmospheric and oceanic modelling*. Report no. 9, 4.33-4.35

Figure 1

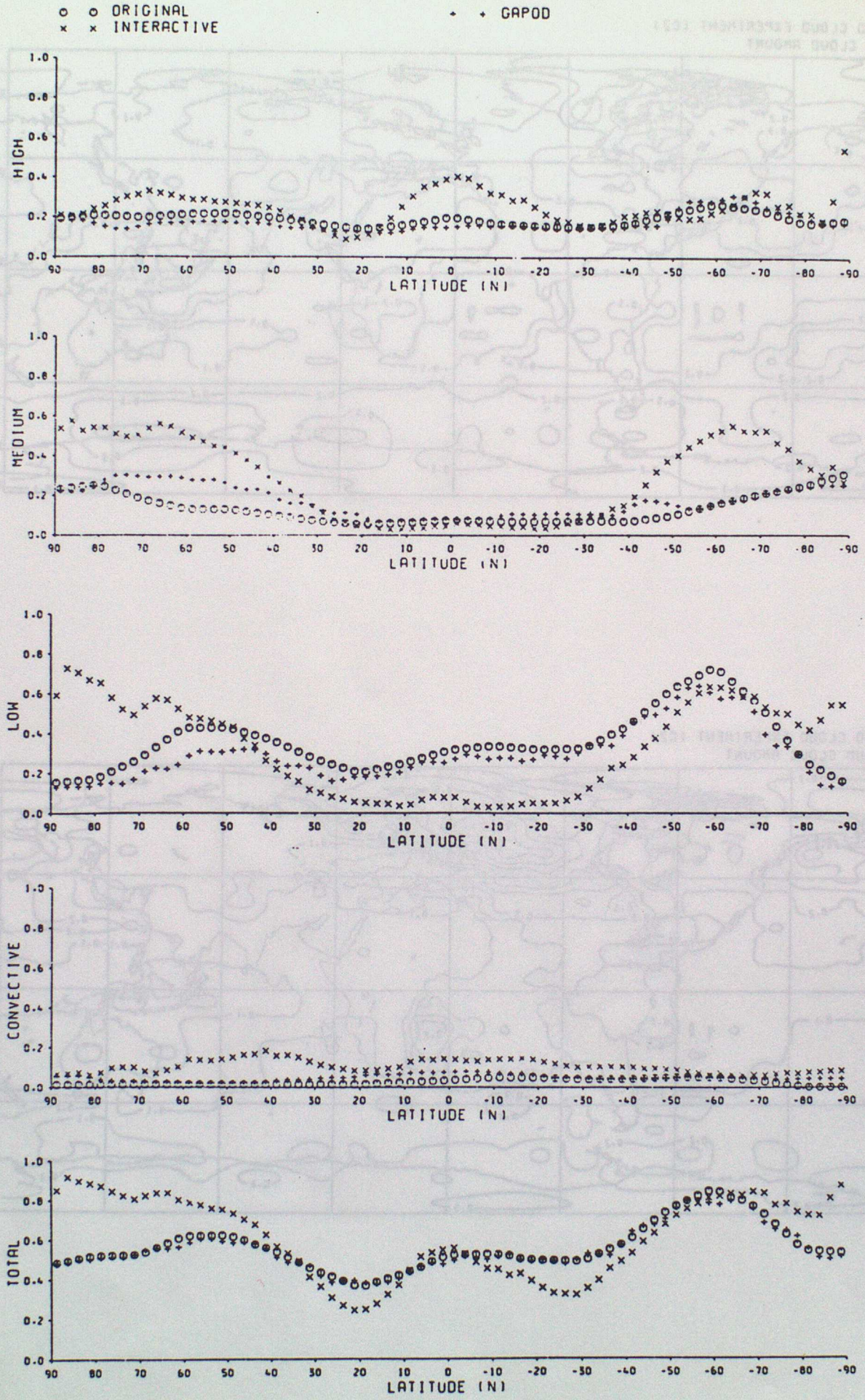
ZONAL MEAN CLOUD AMOUNTS
o o ORIGINAL
× × INTERACTIVE
+ + GAPOD
HIGH
MEDIUM
LOW
CONVECTIVE
TOTAL
1.0
0.8
0.6
0.4
0.2
0.0
90 80 70 60 50 40 30 20 10 0 -10 -20 -30 -40 -50 -60 -70 -80 -90
LATITUDE (N)

Figure 2

a. GAPOD CLOUD EXPERIMENT (C2)
HIGH CLOUD AMOUNT

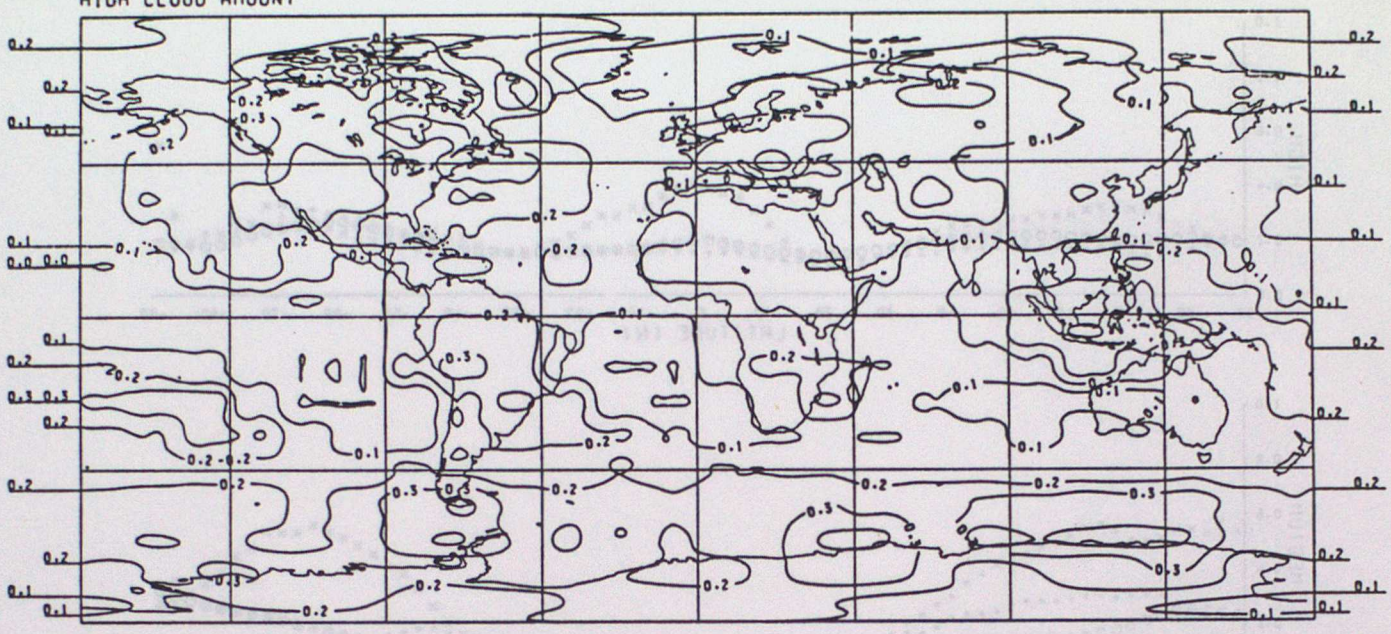

b. GAPOD CLOUD EXPERIMENT (C2)
MEDIUM CLOUD AMOUNT

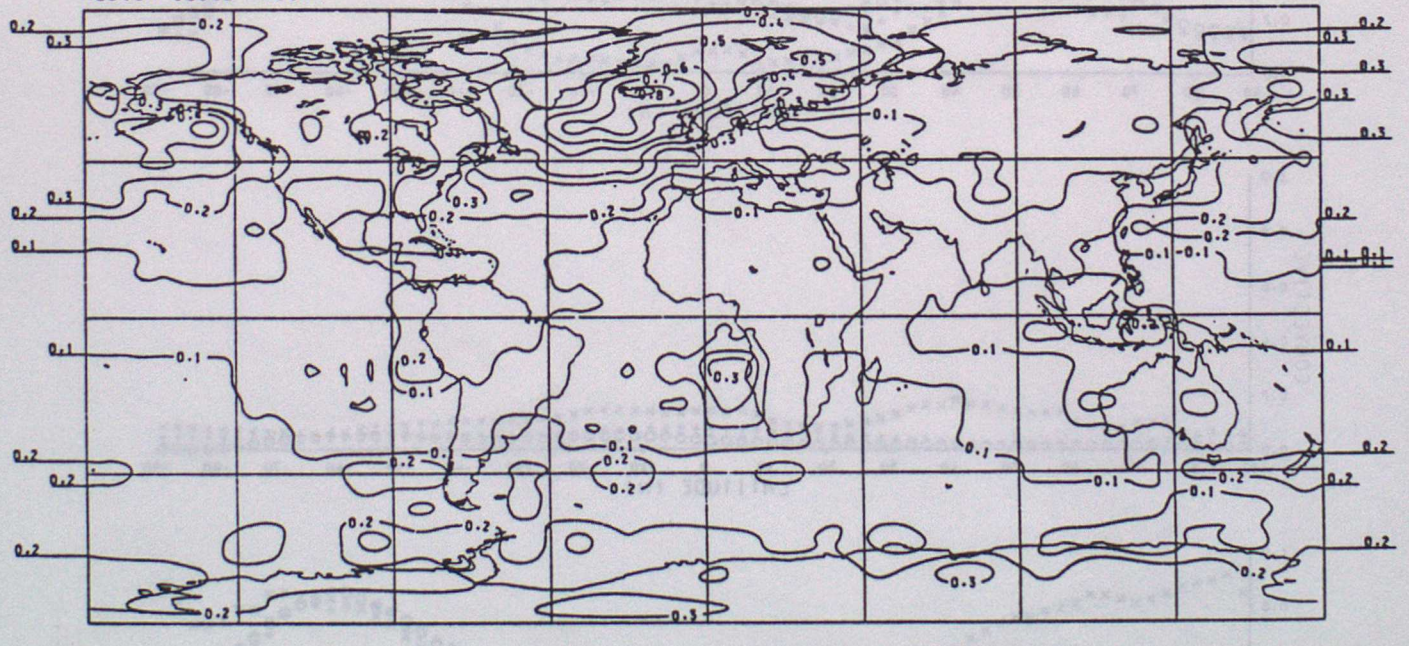

Figure 2 (continued)

c. GAPOD CLOUD EXPERIMENT (C2)
LOW CLOUD AMOUNT

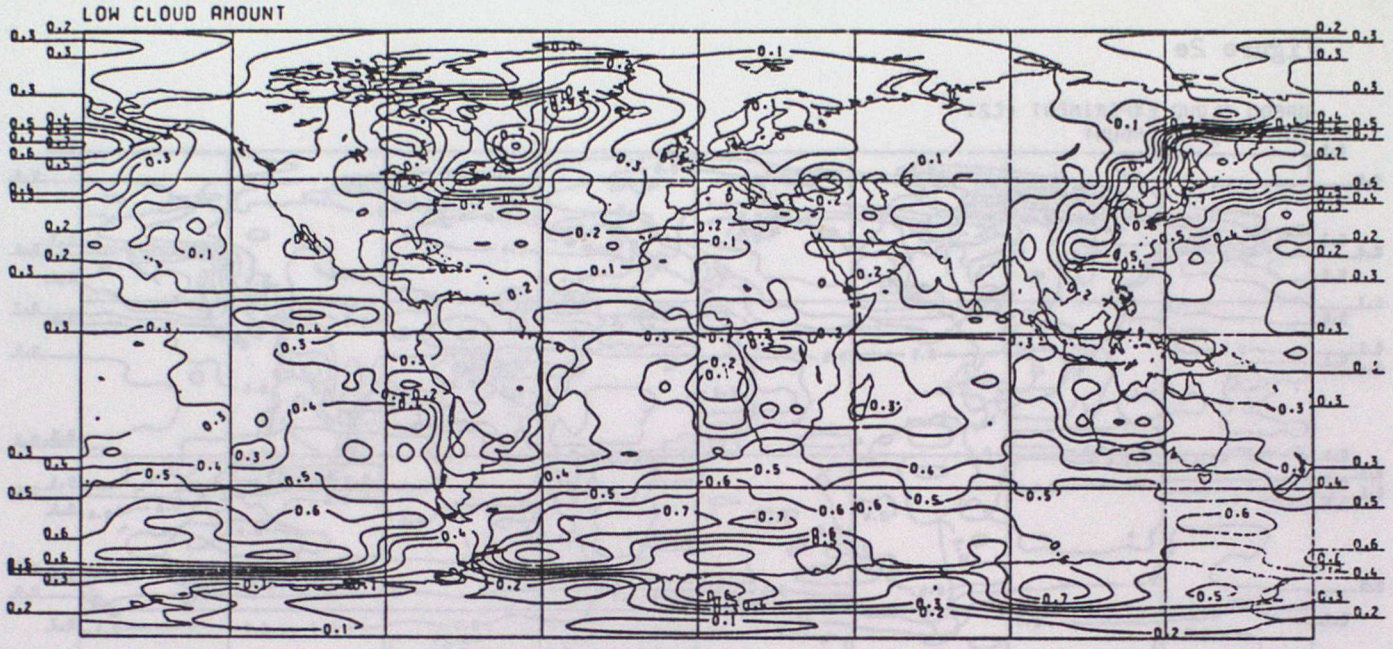

d. GAPOD CLOUD EXPERIMENT (C2)
CONVECTIVE AMOUNT

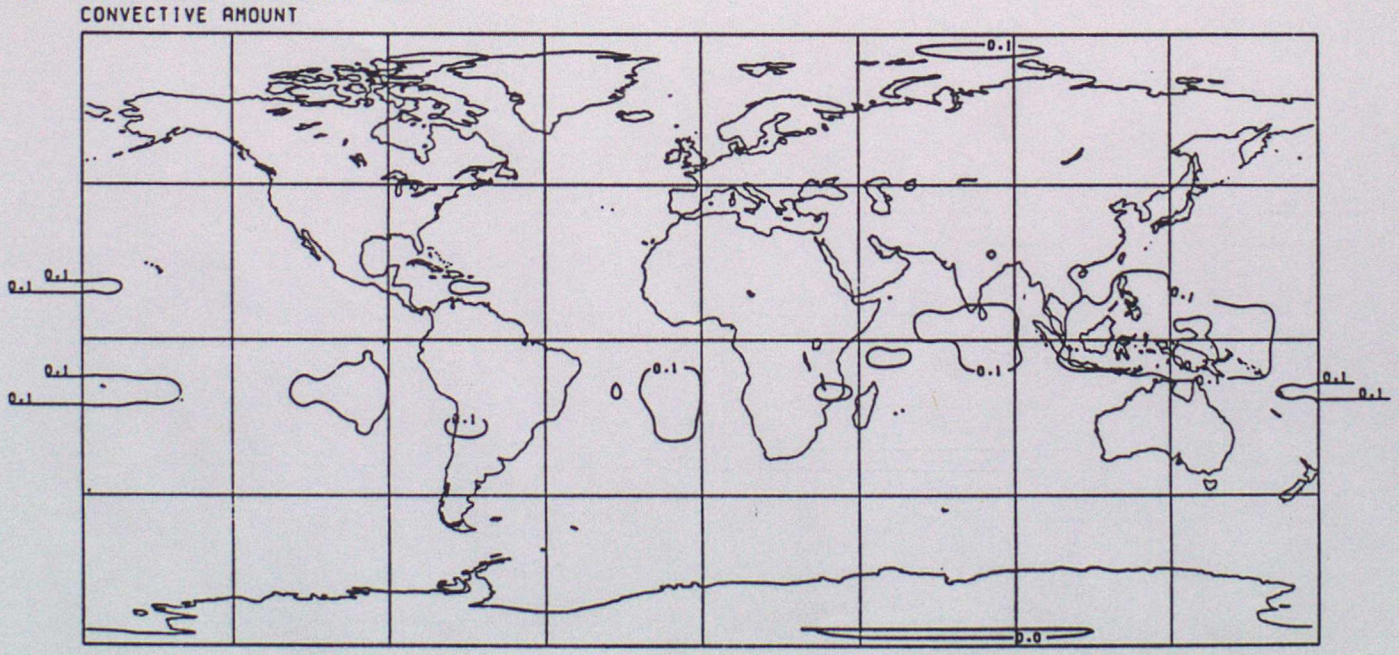

Figure 2e

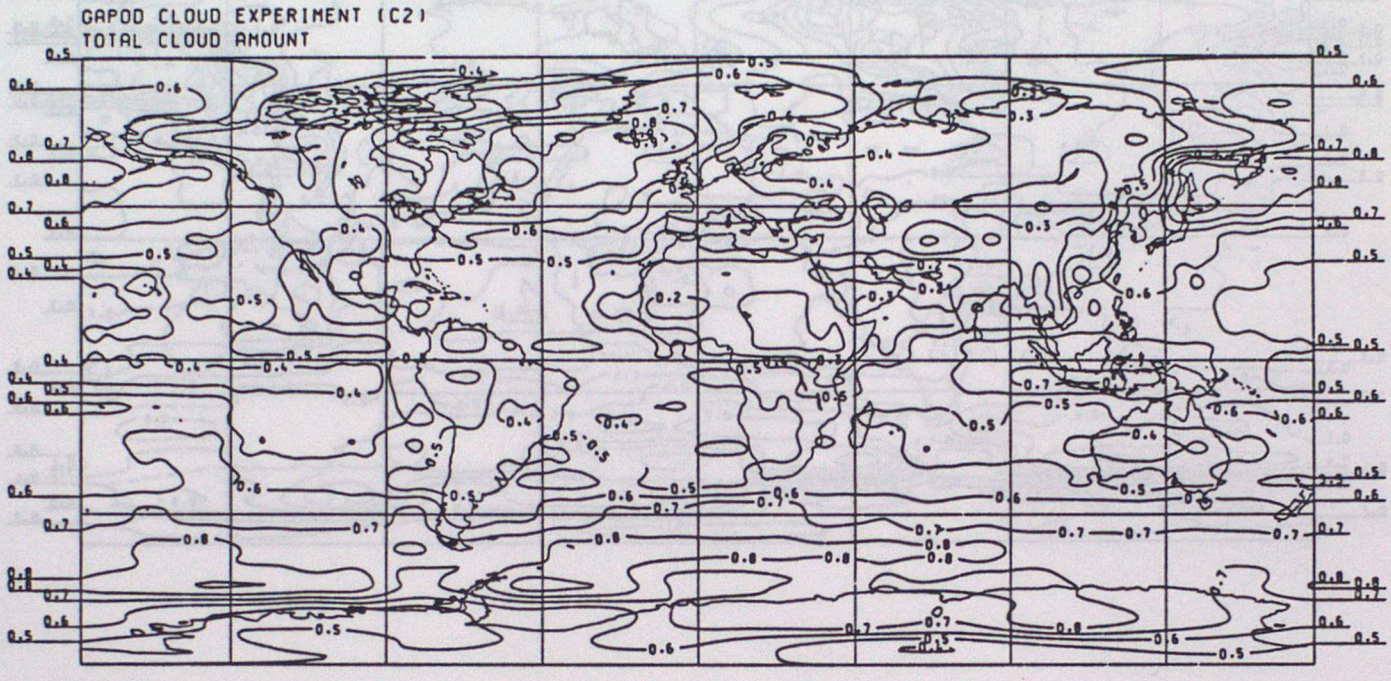

Figure 3

a. INTERACTIVE CLOUD EXPT (C3)
HIGH CLOUD AMOUNT (5 - 2)

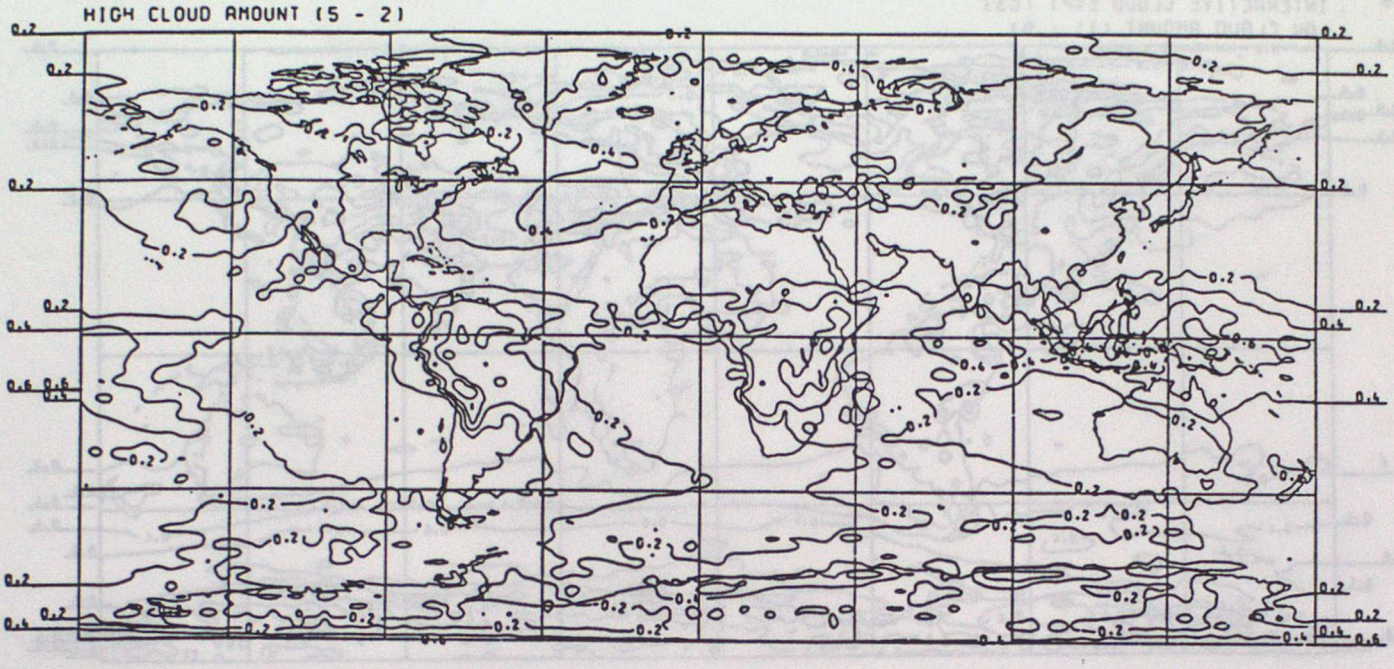

b. INTERACTIVE CLOUD EXPT (C3)
MEDIUM CLOUD AMOUNT (8 - 6)

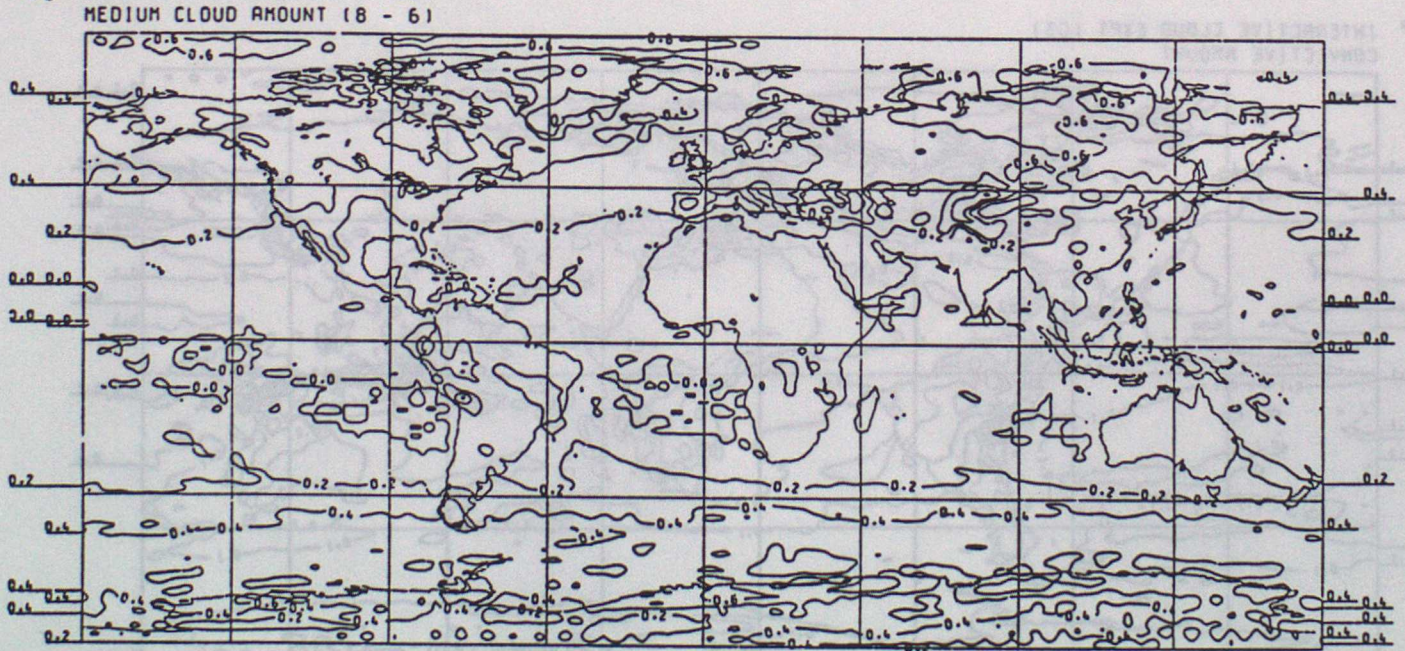

Figure 3 (continued)

c. INTERACTIVE CLOUD EXPT (C3)
LOW CLOUD AMOUNT (11 - 9)

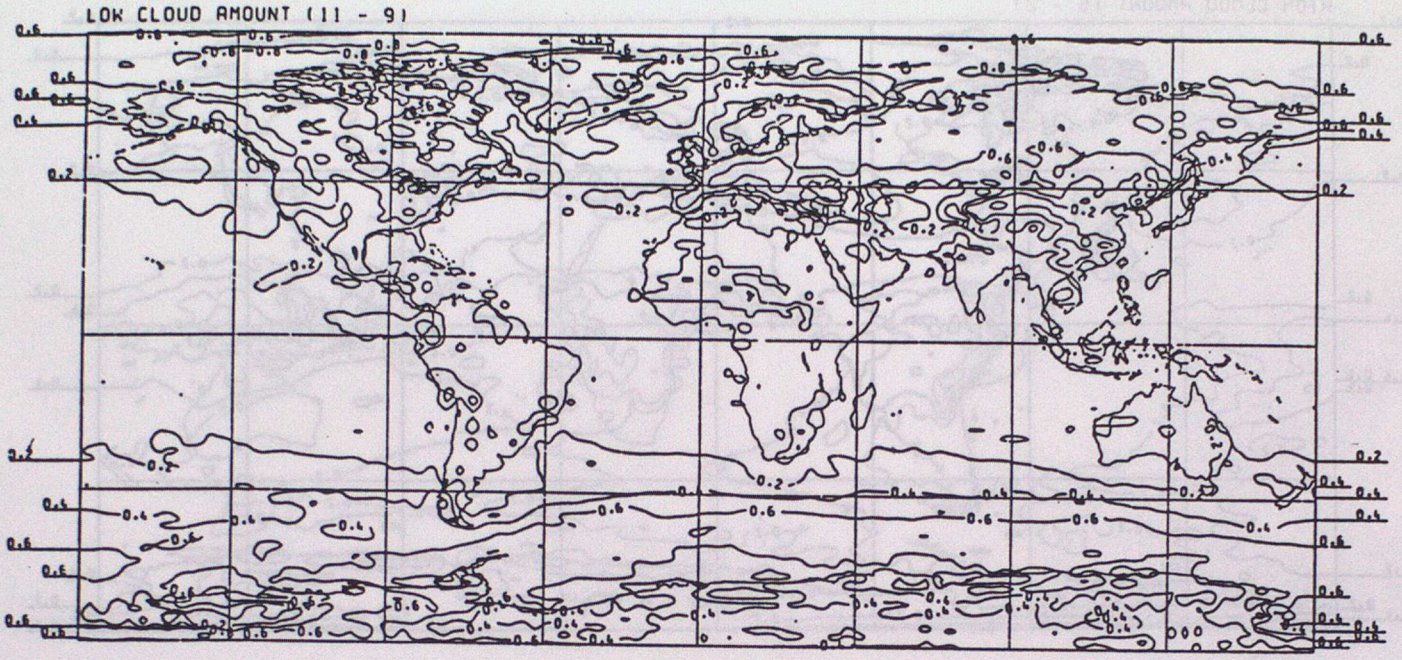

d. INTERACTIVE CLOUD EXPT (C3)
CONVECTIVE AMOUNT

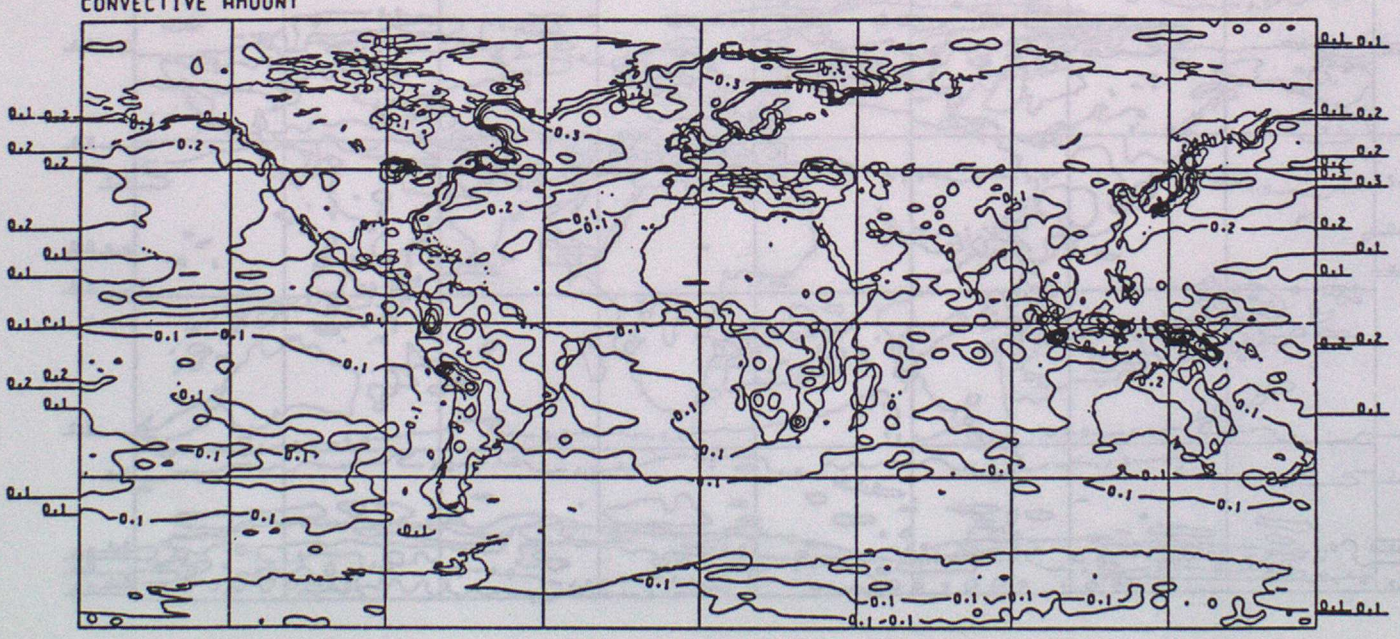

Figure 3 (continued)

e. INTERACTIVE CLOUD EXPT (C3)
SHALLOW CONVECTIVE AMOUNT

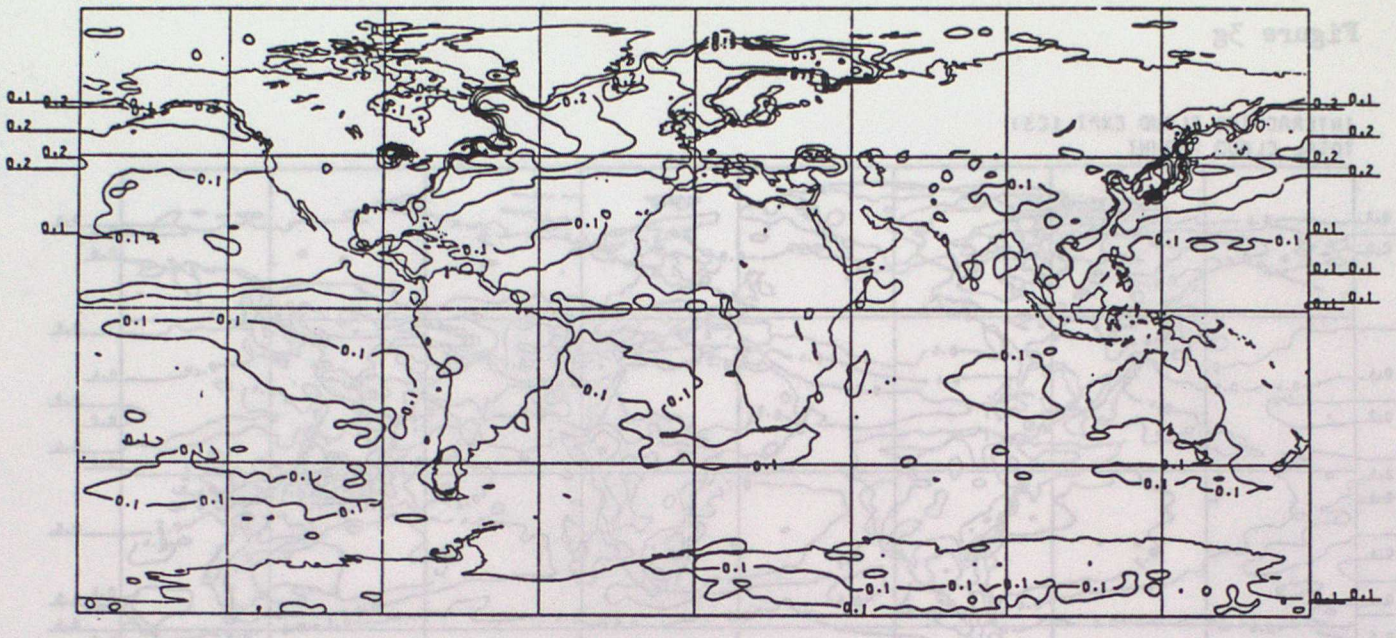

f. INTERACTIVE CLOUD EXPT (C3)
DEEP CONVECTIVE AMOUNT

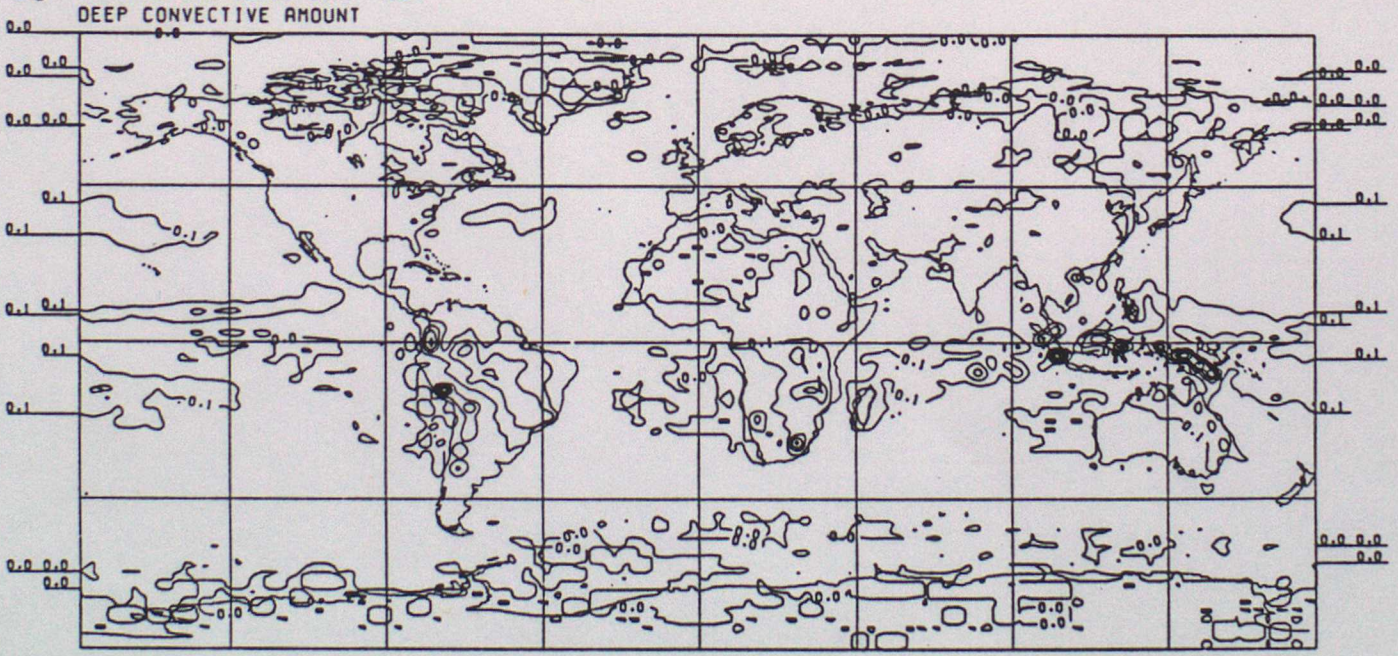

Figure 3g

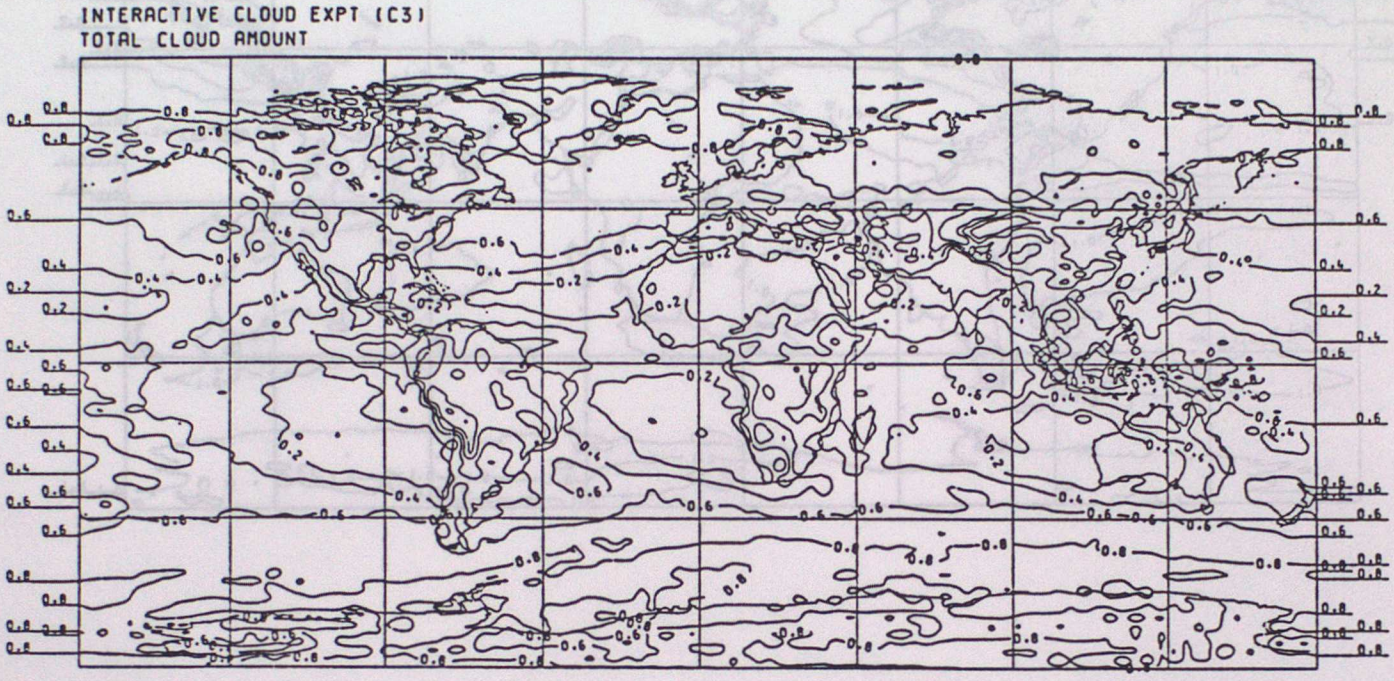

Figure 4

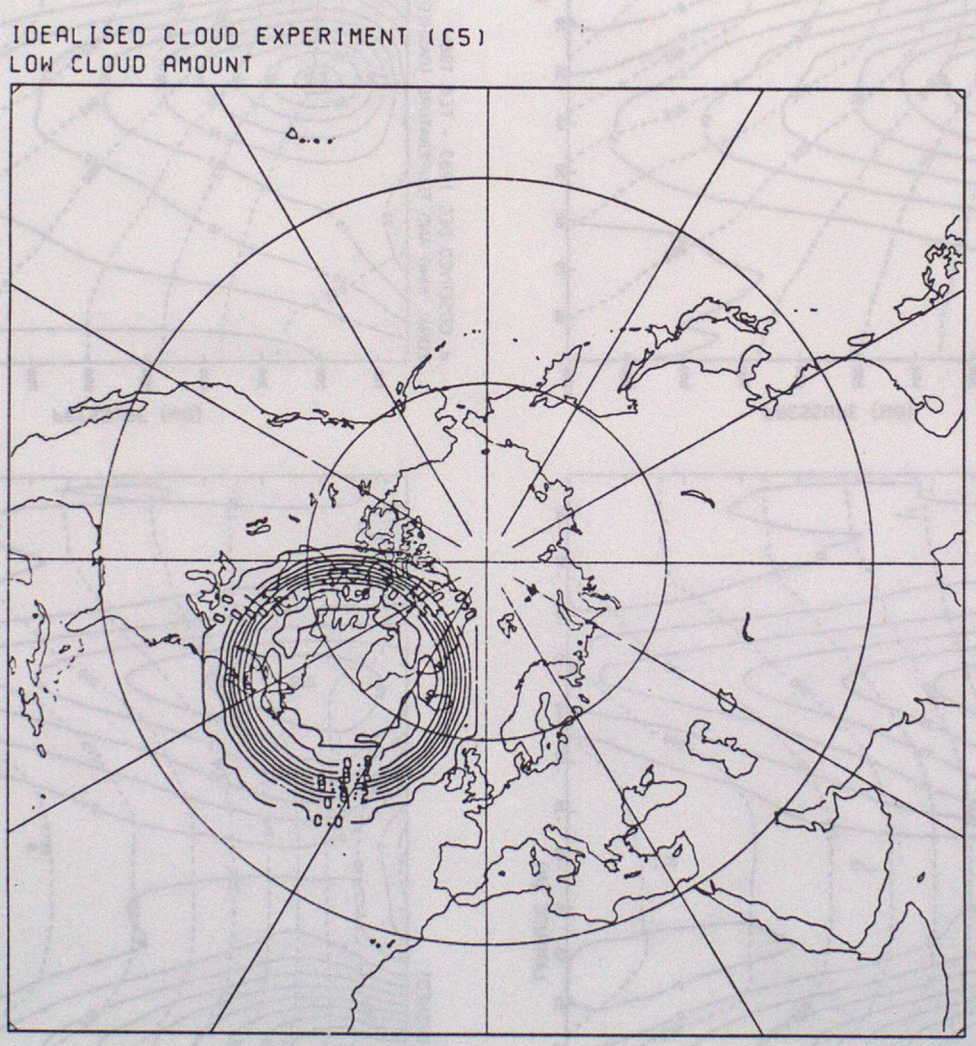

Figure 5

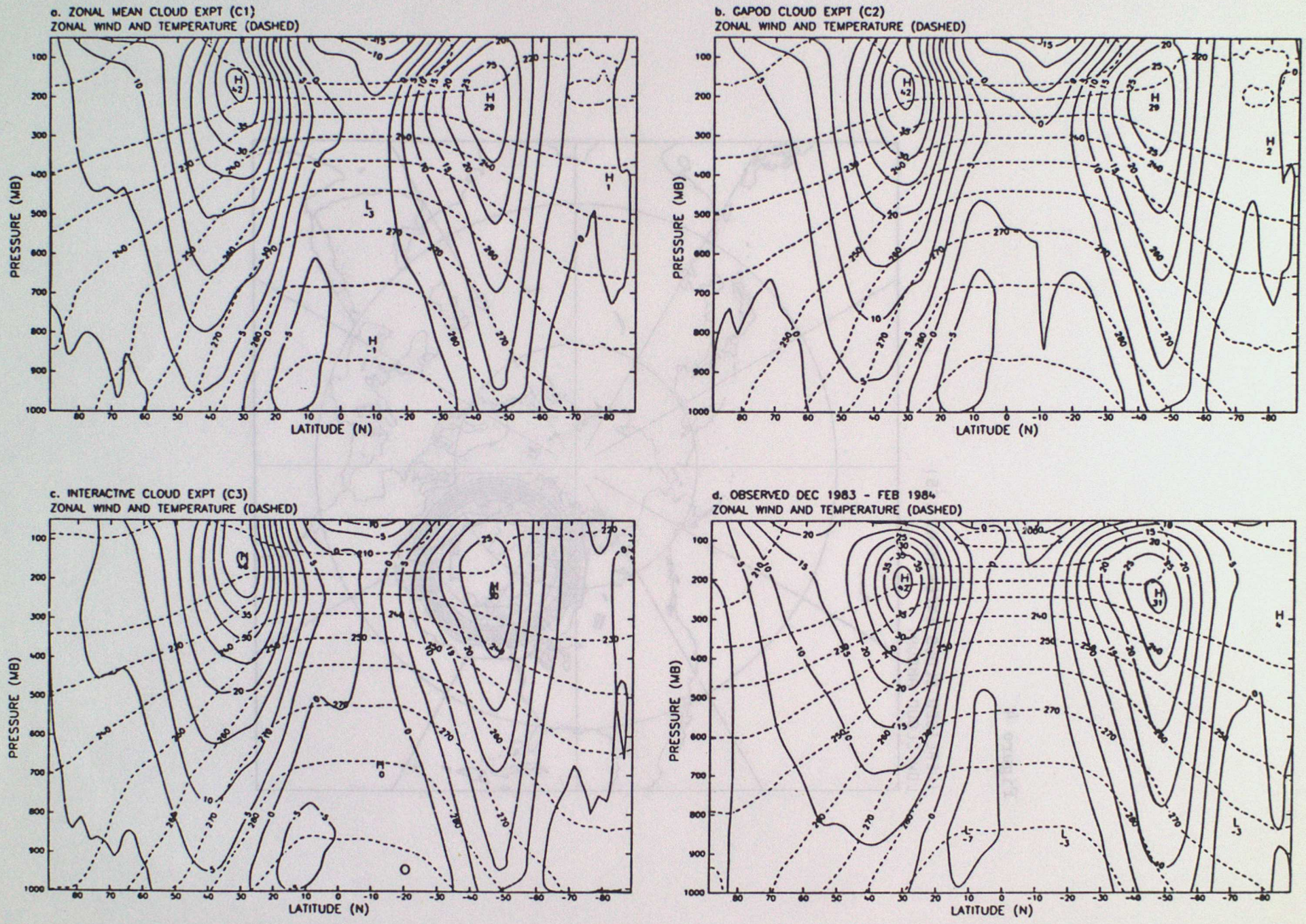
a. ZONAL MEAN CLOUD EXPT (C1)
ZONAL WIND AND TEMPERATURE (DASHED)
b. GAPOD CLOUD EXPT (C2)
ZONAL WIND AND TEMPERATURE (DASHED)
c. INTERACTIVE CLOUD EXPT (C3)
ZONAL WIND AND TEMPERATURE (DASHED)
d. OBSERVED DEC 1983 - FEB 1984
ZONAL WIND AND TEMPERATURE (DASHED)
PRESSURE (MB)
LATITUDE (N)

Figure 6

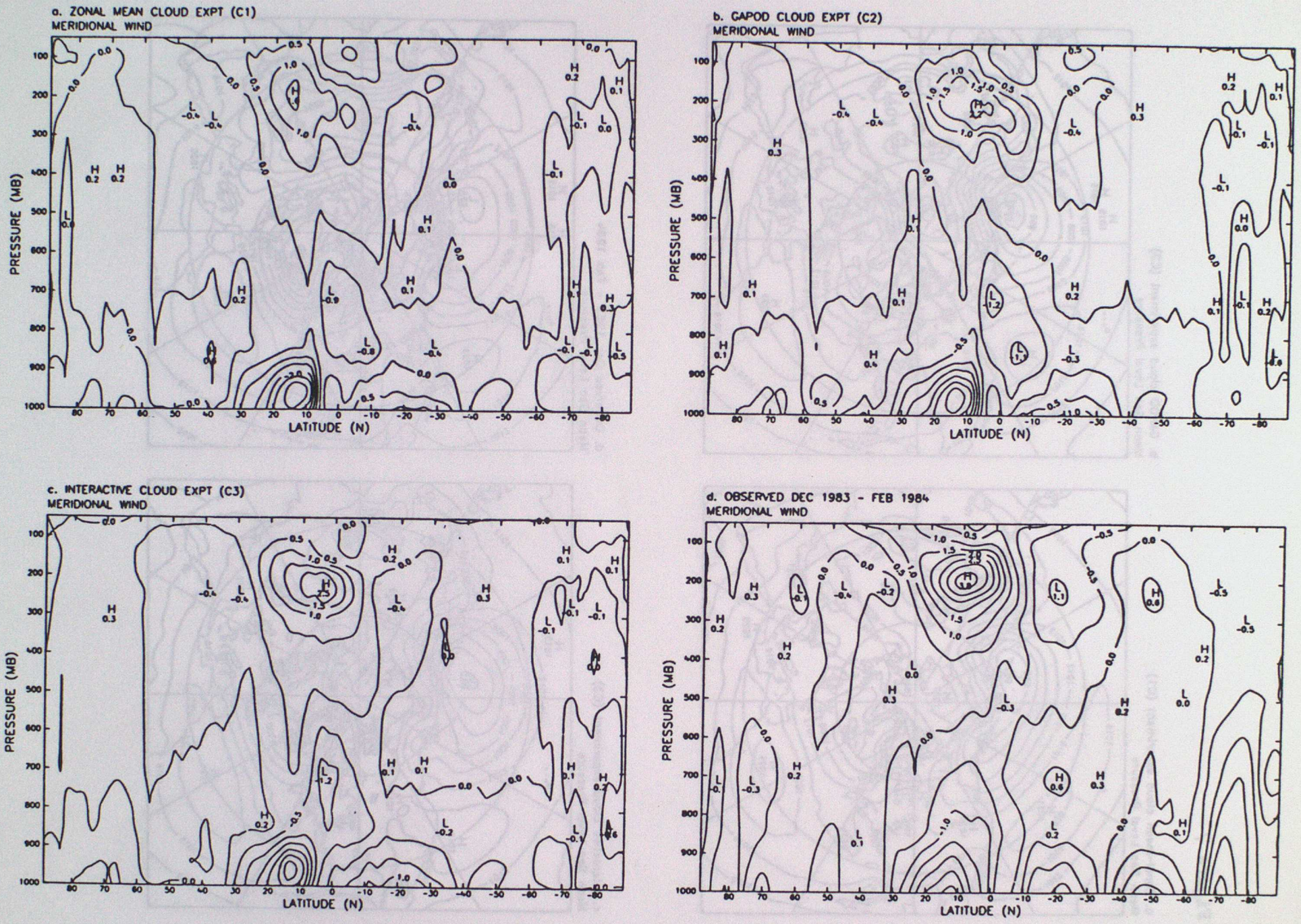
a. ZONAL MEAN CLOUD EXPT (C1)
MERIDIONAL WIND
b. GAPOD CLOUD EXPT (C2)
MERIDIONAL WIND
c. INTERACTIVE CLOUD EXPT (C3)
MERIDIONAL WIND
d. OBSERVED DEC 1983 - FEB 1984
MERIDIONAL WIND
PRESSURE (MB)
LATITUDE (N)

Figure 7

a. Zonal-mean cloud experiment (C1)
Mean Sea Level Pressure

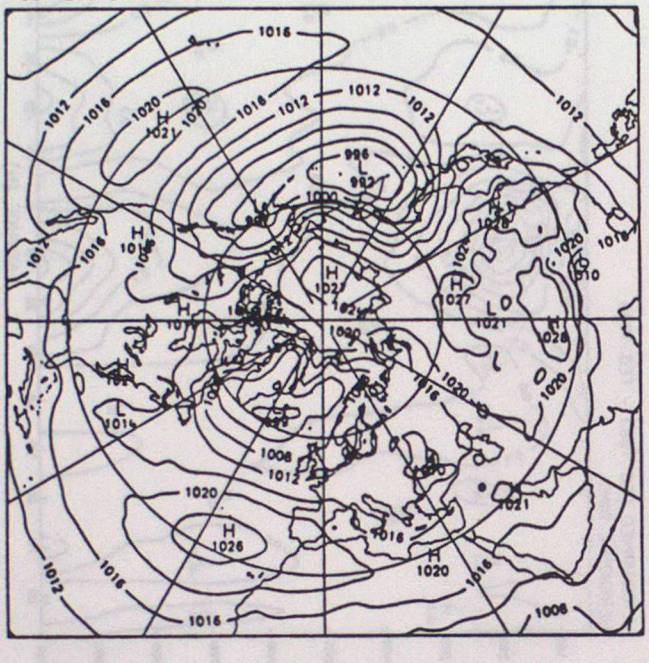

b. GAPOD cloud experiment (C2)
Mean Sea Level Pressure

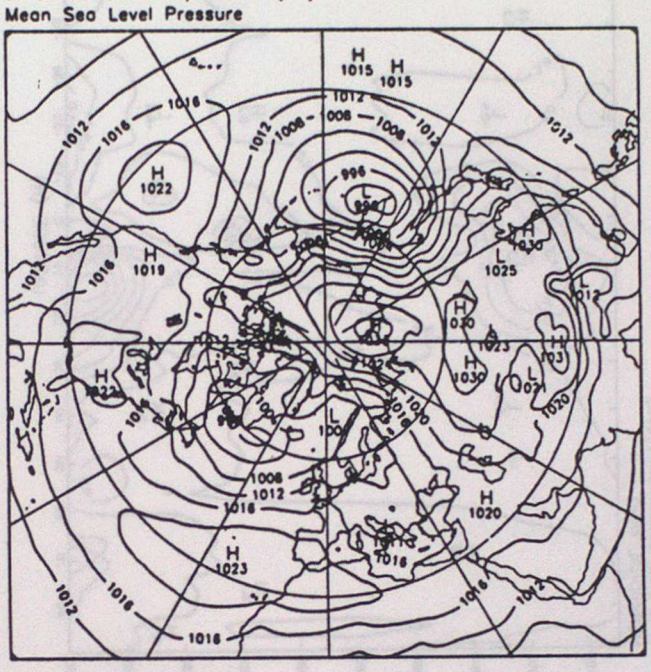

c. Interactive cloud experiment (C3)
Mean Sea Level Pressure

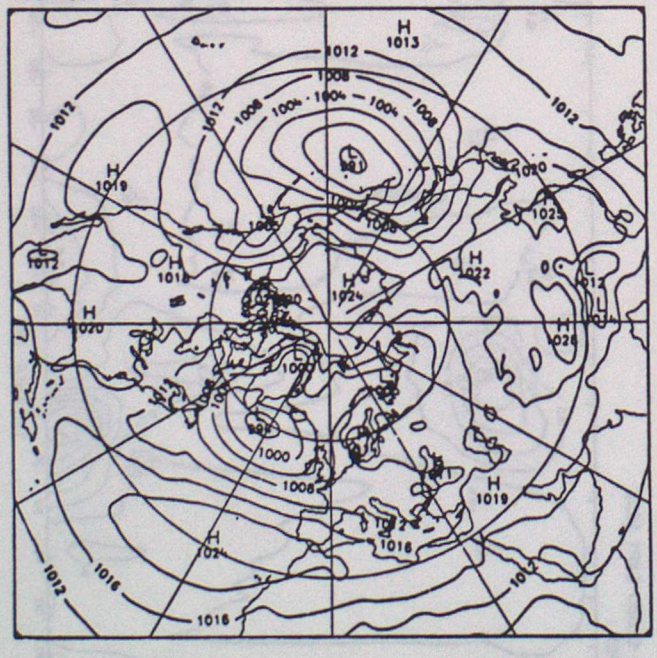

d. Observed Dec 1983 - Feb 1984
Mean Sea Level Pressure

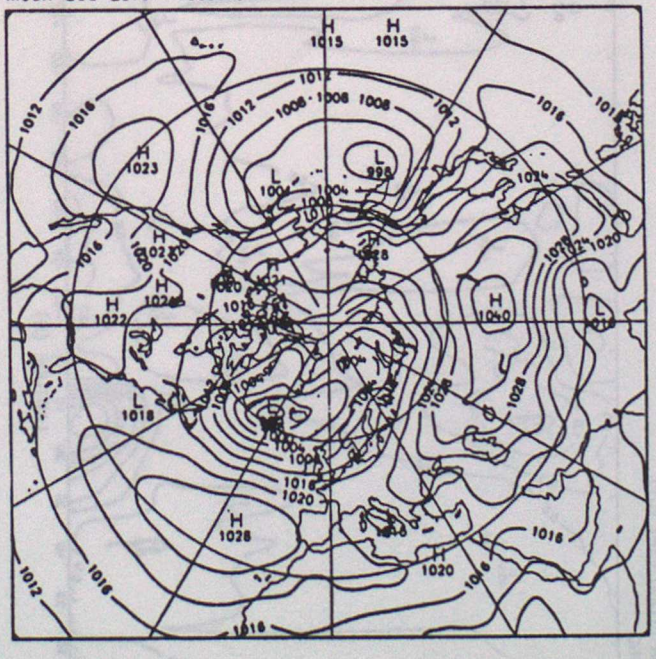

Figure 8

a. Zonal-mean cloud experiment (C1)
High-pass filtered RMS 500 mb Height

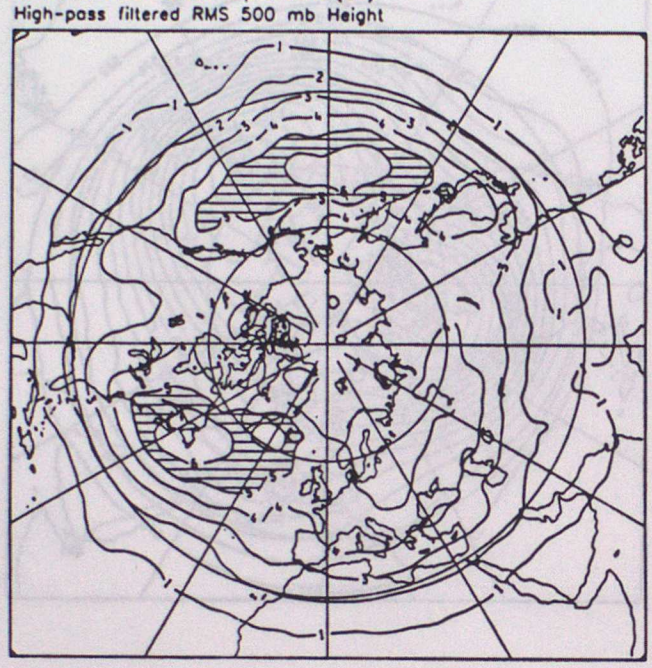

b. GAPOD cloud experiment (C2)
High-pass filtered RMS 500 mb Height

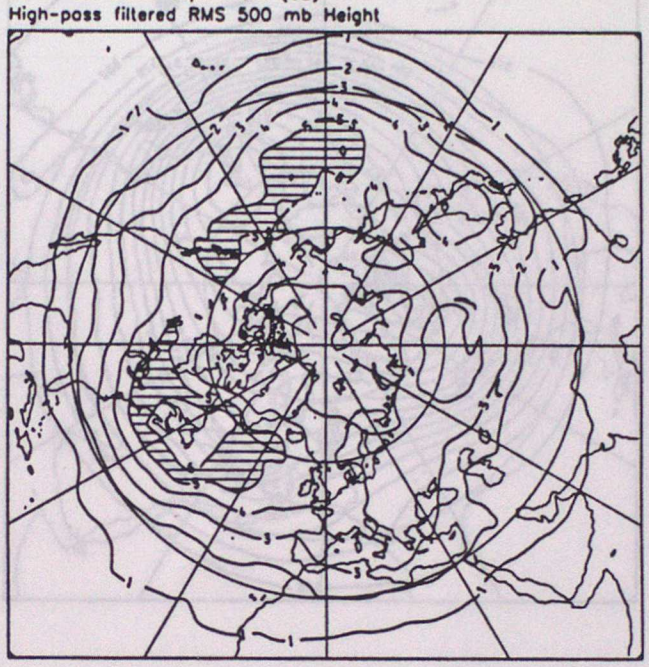

c. Interactive cloud experiment (C3)
High-pass filtered RMS 500 mb Height

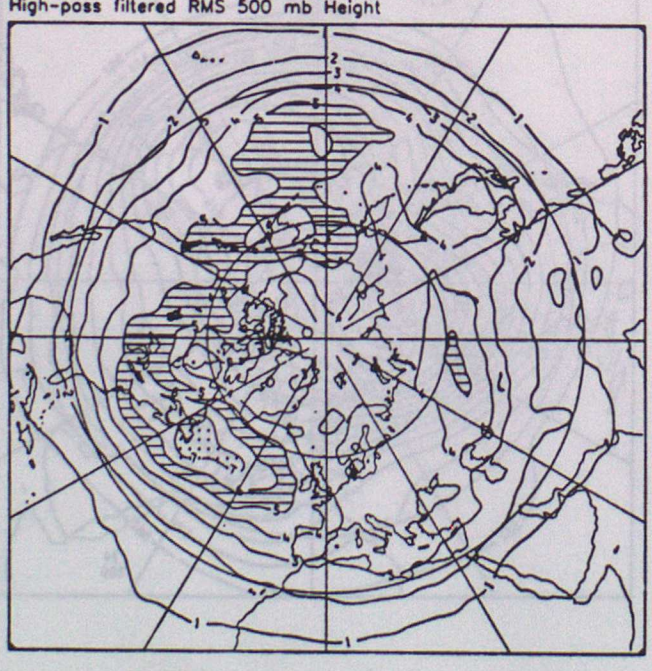

d. Observed Dec 1983 - Feb 1984
High-pass filtered RMS 500 mb Height

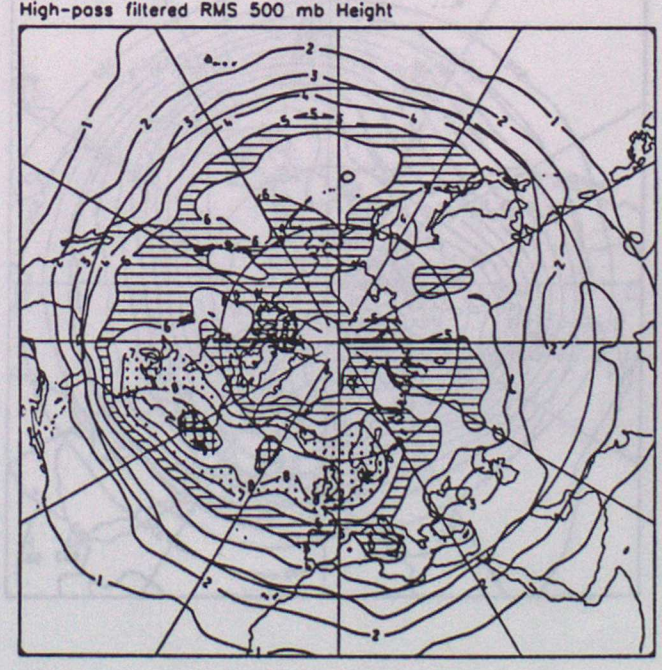

Figure 9

a. Zonal-mean cloud experiment (C1)
500 mb Height

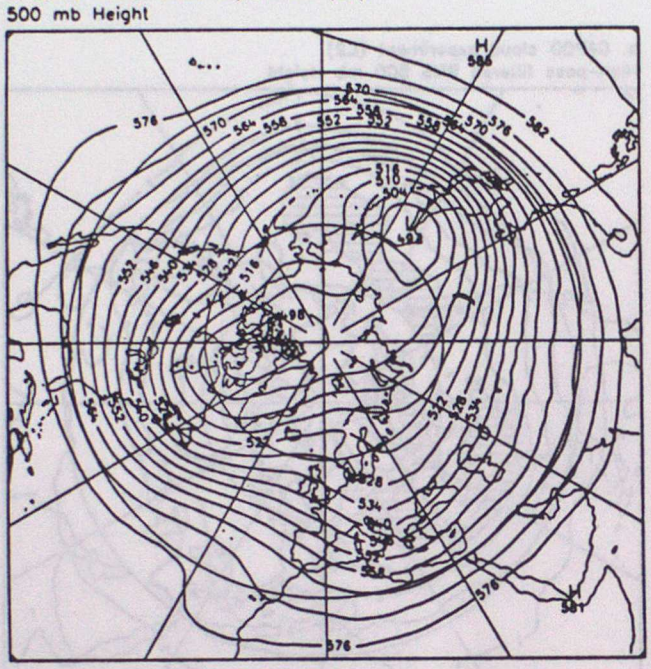

b. GAPOD cloud experiment (C2)
500 mb Height

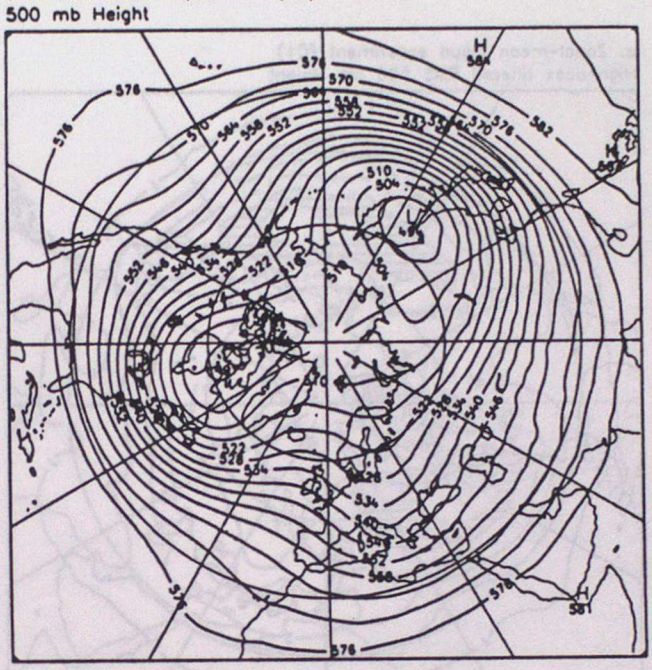

c. Interactive cloud experiment (C3)
500 mb Height

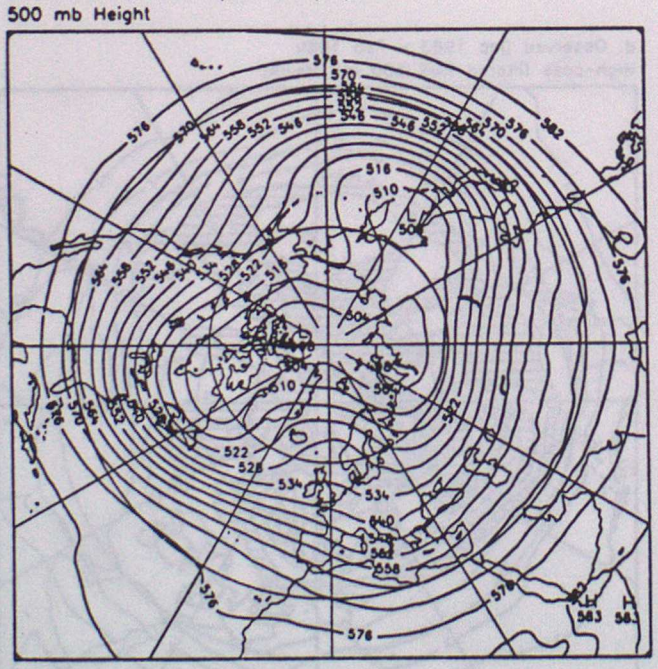

d. Observed Dec 1983 - Feb 1984
500 mb Height

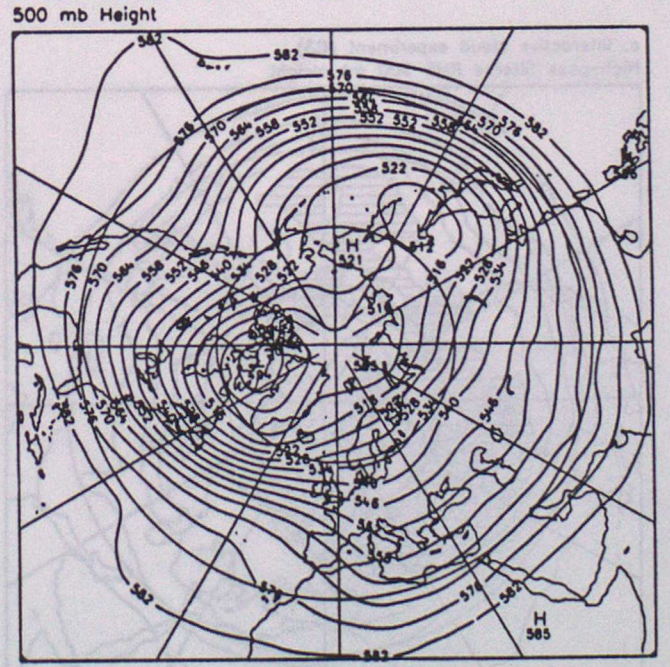

Figure 10

a. No-cloud experiment (C4)
Mean Sea Level Pressure

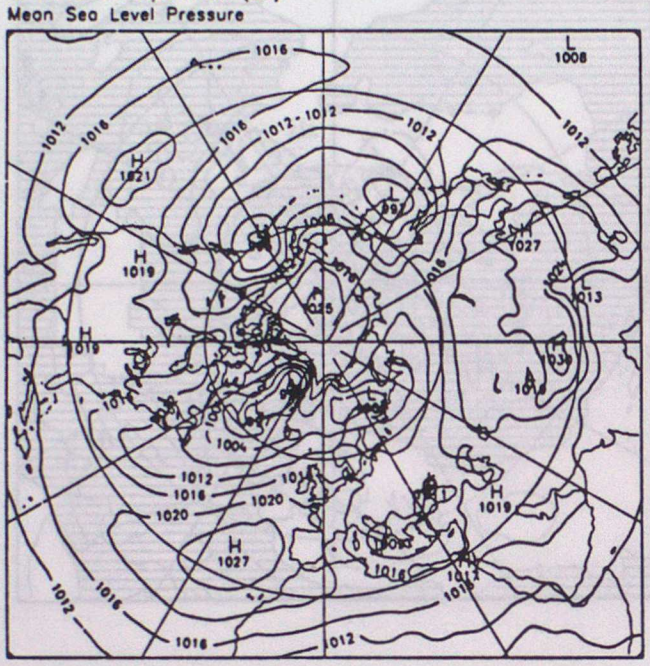

b. Idealised cloud experiment (C5)
Mean Sea Level Pressure

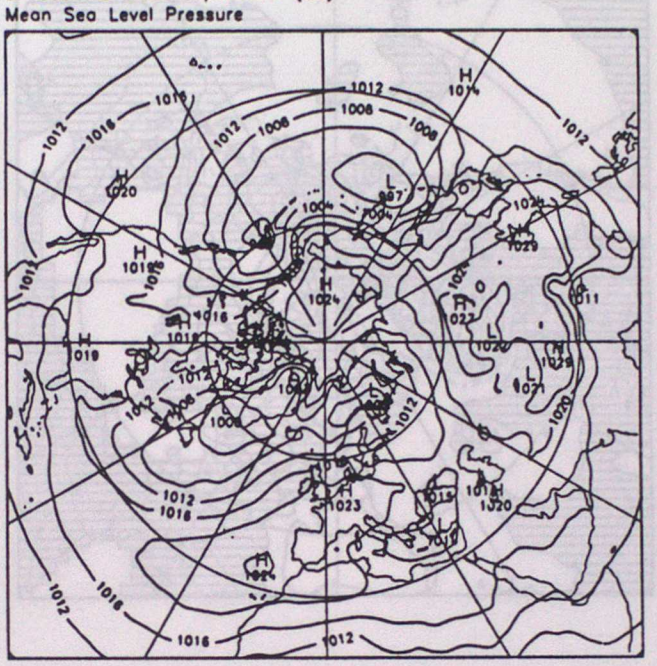

c. Difference C5 minus C4
Mean Sea Level Pressure

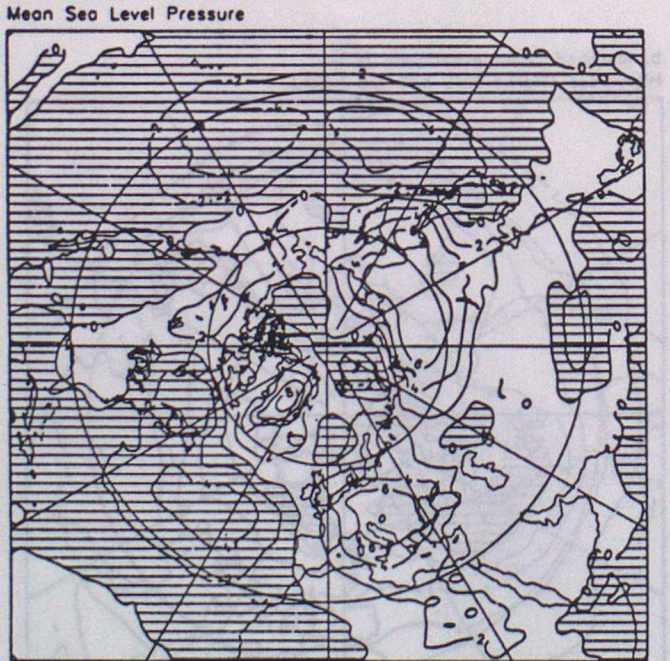

Figure 11

Idealised cloud (C5) minus no cloud (C4)
850 mb Temperature difference

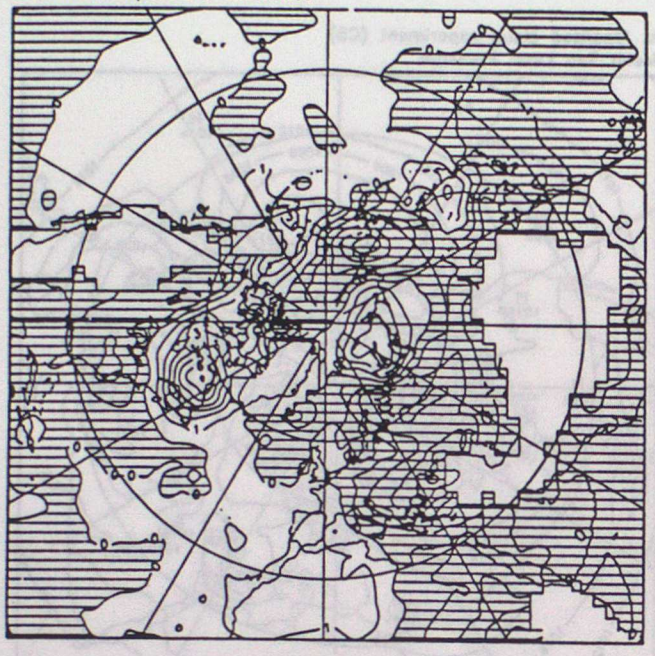

Idealised cloud (C5) minus no cloud (C4)
700 mb Temperature difference

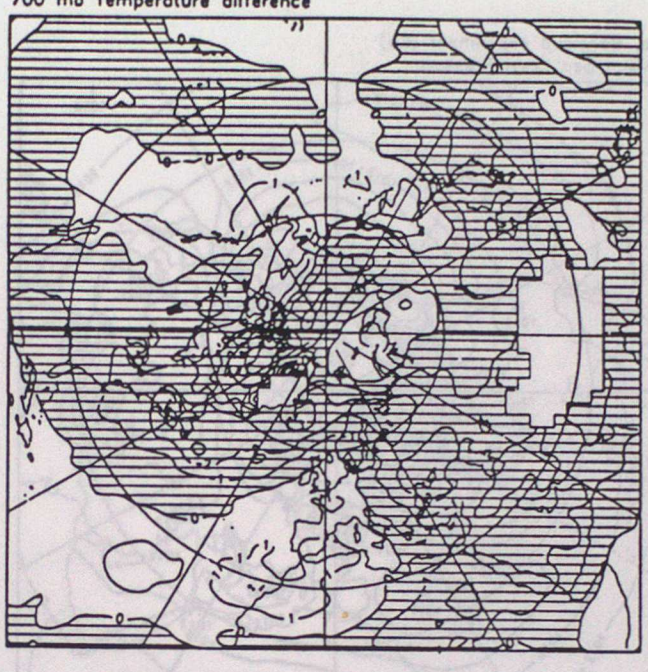

Figure 12

a. No-cloud experiment (C4)
High-pass filtered RMS 500 mb height

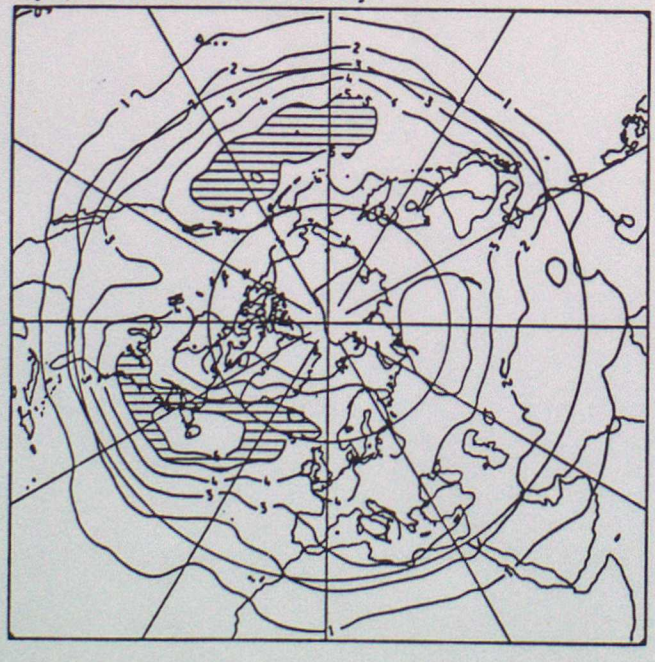

b. Idealised cloud experiment (C5)
High-pass filtered RMS 500 mb height

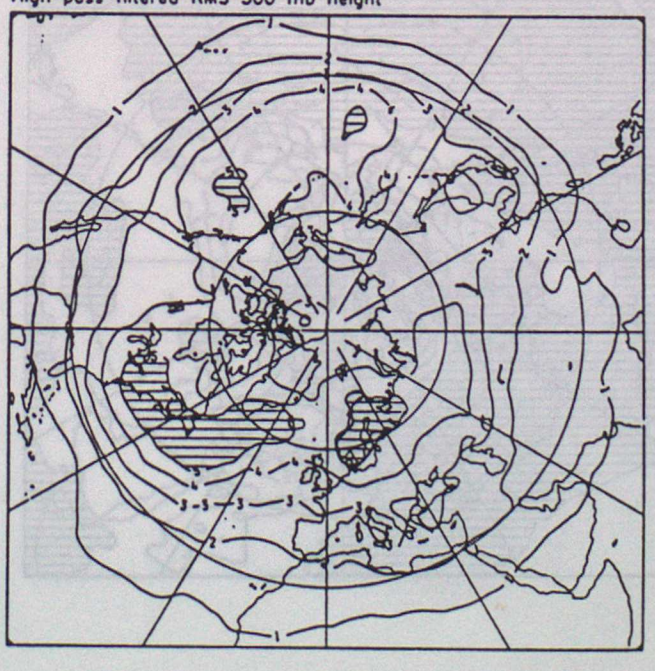

Figure 13

a. No-cloud experiment (C4)
500 mb Height

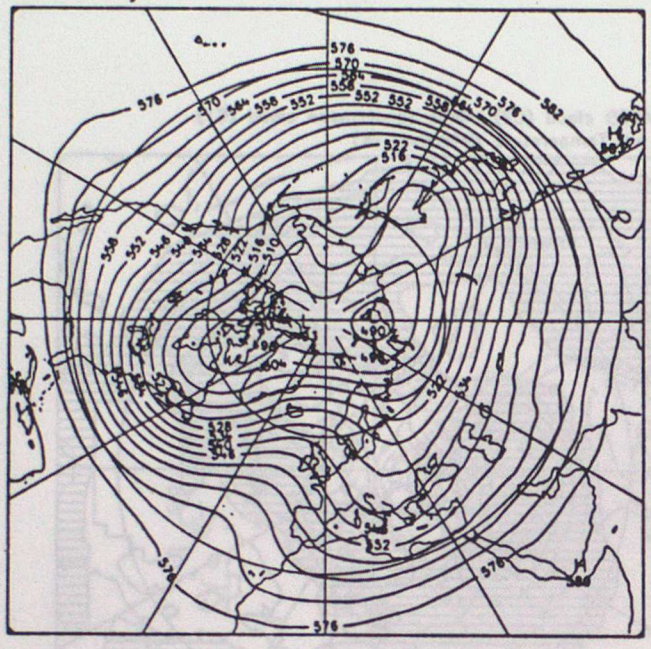

b. Idealised cloud experiment (C5)
500 mb Height

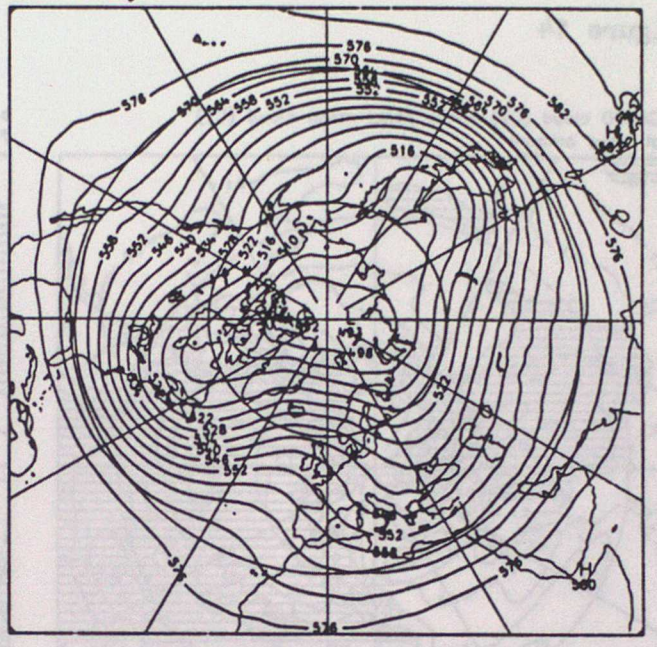

c. Difference C5 minus C4
500 mb Height

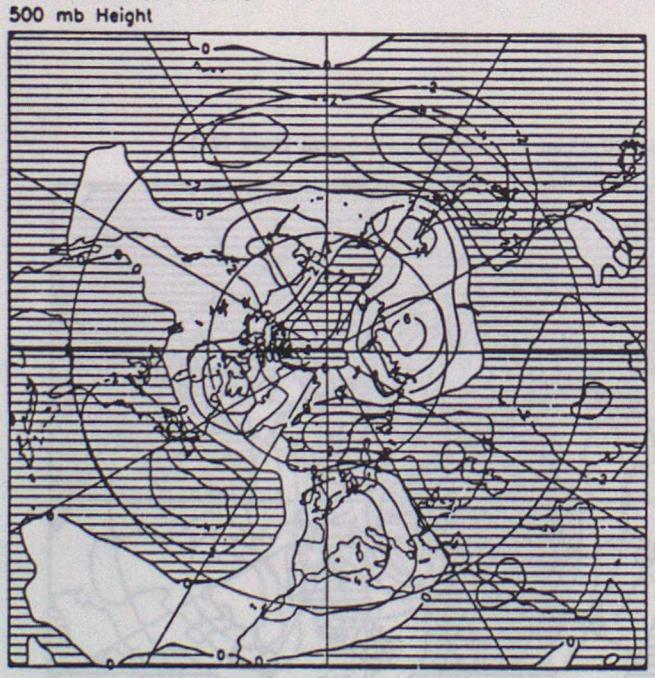

Figure 14

a. GAPOD cloud (C2) minus zonal-mean cloud (C1)
Total cloud amount

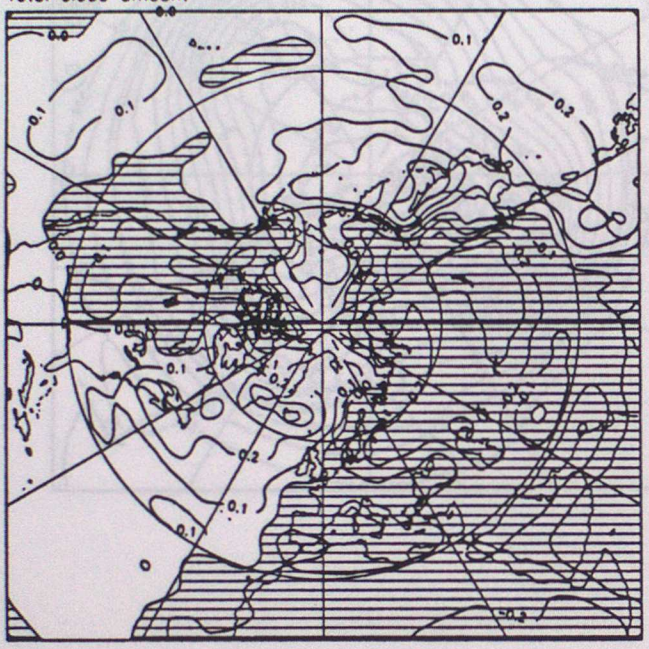

b. GAPOD cloud (C2) minus zonal-mean cloud (C1)
700 mb Temperature difference (K)

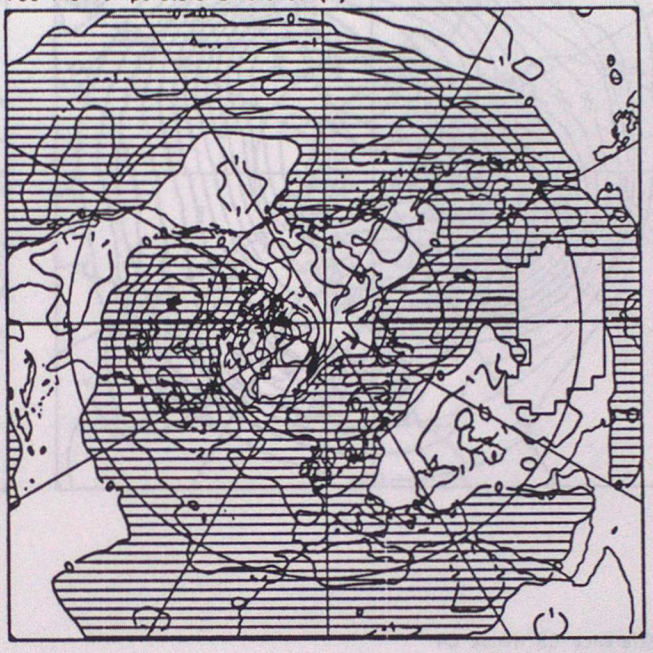

c. GAPOD cloud (C2) minus zonal-mean cloud (C1)
Mean sea level Pressure (mb)

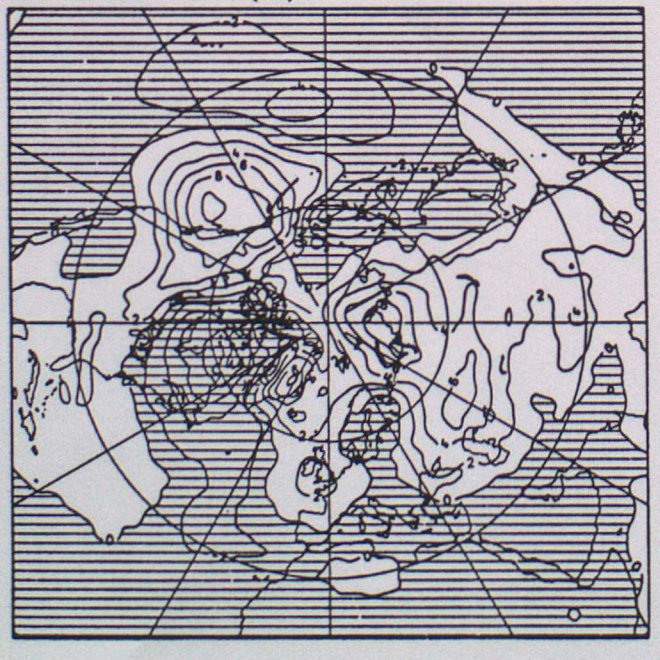

d. GAPOD cloud (C2) minus zonal-mean cloud (C1)
500 mb Geopotential height (Dm)

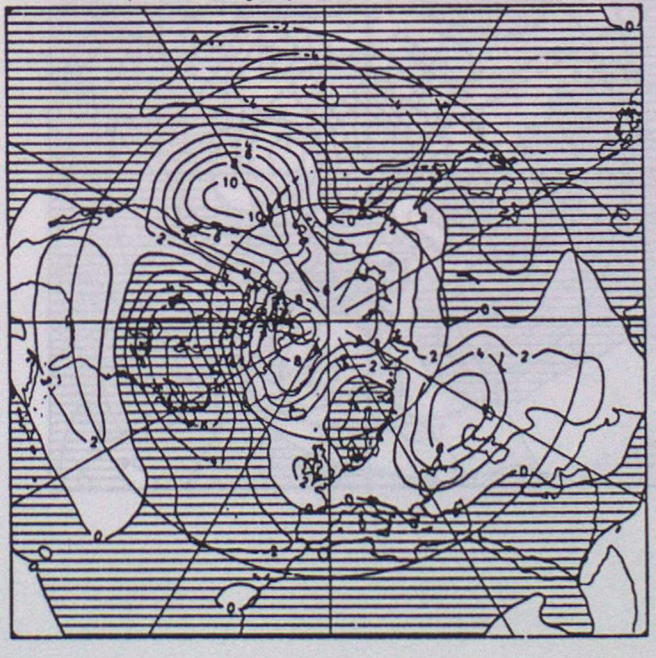

INDEX TO LONG-RANGE FORECASTING AND CLIMATE RESEARCH SERIES

1. THE CLIMATE OF THE WORLD - Introduction and description of world climate.
   by C K Folland (March 1986)

2. THE CLIMATE OF THE WORLD - Forcing and feedback processess.
   by C K Folland (March 1986)

3. THE CLIMATE OF THE WORLD - El Nino/Southern Oscillation and the Quasi-biennial Oscillation.
   by C K Folland and D E Parker (March 1986)

4. THE CLIMATE OF THE WORLD - Climate change: the ancient earth to the 'Little Ice Age'.
   by C K Folland (March 1986)

5. THE CLIMATE OF THE WORLD - Climate Change: the instrumental period.
   by C K Folland and D E Parker (March 1986)

6. THE CLIMATE OF THE WORLD - Carbon dioxide and climate (with appendix on simple climate models).
   by D E Parker, C K Folland and D J Carson (March 1986)

7. Sahel rainfall, Northern Hemisphere circulation anomalies and worldwide sea temperature changes. (To be published in the Proceedings of the "Pontifical Academy of Sciences Study Week", Vatican, 23-27 September 1986).
   by C K Folland, D E Parker, M N Ward and A W Colman (September 1986)

8. Lagged-average forecast experiments with a 5-level general circulation model.
   by J M Murphy (March 1986)

9. Statistical Aspects of Ensemble Forecasts.
   by J M Murphy (July 1986)

10. The Impact of El Nino on an Ensemble of Extended-Range Forecasts. (Submitted to Monthly Weather Review)
    by J A Owen and T N Palmer (December 1986)

11. An experimental forecast of the 1987 rainfall in the Northern Nordeste region of Brazil.
    by M N Ward, S Brooks and C K Folland (March 1987)

12. The Sensitivity of Estimates of Trends of Global and Hemisphere Marine Temperature to Limitations in Geographical Coverage.
    by D E Parker (April 1987)

13. General circulation model simulations using cloud distributions from the GAPOD satellite data archive and other sources.
    by R Swinbank (May 1987)

14. Simulation of the Madden and Julian Oscillation in GCM experiments.
    by R Swinbank (May 1987)